PENETRABILITY THROUGH DOUBLE HUMP BARRIERS IN NUCLEAR FISSION PROCESSES

Jean-Nöel G.M. Leboeuf

A THESIS

in

Physics

Presented in Partial Fulfillment of the Requirements for the
Degree of Master of Science at
Sir George Williams University
Montreal, Canada

September, 1972

ABSTRACT

The penetrability through double hump barriers in nuclear fission processes is calculated in the J.W.K.B. approximation, using Fröman's "F-Matrix" formalism. Particular attention is paid to coinciding classical turning points where other methods break down. An attempt is made to obtain a more realistic picture by introducing the "Sharp Drop Approximation" to modify Cramer and Nix's method of calculating penetrabilities. An expression for the penetrability through two-peaked fission barriers is obtained in terms of Weber parabolic cylinder functions. A qualitative discussion of results is also included.

ACKNOWLEDGEMENTS

The author would like to thank Dr. R.C. Sharma for his assistance and constant encouragement throughout this work. He also is deeply indebted to the National Research Council for financial assistance during the course of this research. Finally, the author would like to thank his wife, for her moral support and her understanding during the period that this work was carried out.

TABLE OF CONTENTS

TABLE OF CONTENTS (Continued)

TABLE OF CONTENTS (Continued)

TABLE OF CONTENTS (Continued)

LIST OF FIGURES

LIST OF FIGURES (Continued)

INTRODUCTION

INTRODUCTION

PENETRABILITY THROUGH DOUBLE HUMP BARRIER IN NUCLEAR FISSION PROCESS

The fortuitous experimental discovery of nuclear fission by O.Hahn and F. Strasseman,[1] in 1939 presented a challenge to theoretical physicists. They realized that fission, a many-body phenomenon, would be a formidable problem to solve exactly with quantum mechanics, both in its statical and dynamical aspects. This prompted researchers to fit a model to the physical situation. On suggestions from L. Meitner and O.R. Frisch,[2] Bohr and Wheeler[7] developed the Liquid Drop Model. Unfortunately, this very simple model is only a rough approximation of the fission mechanism. However, it provides a reasonable qualitative picture of break up of the nucleus. The Liquid Drop Model was soon superceded by Bohr and Mottelson's [12] Unified or Collective Model. It was an advance in sophistication since it included single particle degrees of freedom. Nevertheless, it has been extremely difficult to apply this model quantitatively to fission. A. Bohr's [16] channel theory was one of the few attempts, which succeeded in explaining the importance of the saddle point and gave a useful expression for the angular distribution of fission fragments. It still remained to be seen if shell effects would influence the fission phenomenon as strongly as was hoped in the advent of the theory, since shells

seemed to disappear in highly deformed nuclei. Strutinsky[20] found a way to include shell effects consistently in nuclear masses and deformation energies through the Shell Correction Method. When Shell Correction is applied to the variation of nuclear masses with deformation, i.e. to fission, in the limit, it yields an unusual result. The fission barrier was then thought to include only one potential maximum corresponding to the saddle point energy. Strutinsky [24] however, obtained a fission barrier consisting of two energy minima separated by an intermediate well. Thus the saddle point was more intricate than expected.

Since the fission barrier is primarily used to estimate fission half-lives, the penetrability of the barrier, in terms of which the fission half-life is expressed, has to be considered with the utmost care. The probability of penetration through Strutinsky's fission barrier is calculated in the J.W.K.B. approximation in Chapter IV. A preliminary calculation is carried out with the J.W.K.B. method as understood by Bohm [38] and others. In this Chapter, the author derives a result often quoted. However, Fröman[39] proved that Bohm's view of the J.W.K.B. approximation is mathematically erroneous. In our opinion, the expression for the penetrability mostly used lacks mathematical rigor. The author gives a mathematically rigorous derivation of the penetrability in the J.W.K.B. approximation using Fröman's point of view of J.W.K.B. method.

Furthermore, the problem of calculating the penetrability of a fission barrier when the incident energy is close to the top of the barrier has not yet been attempted for the case of a double-hump asymmetric barrier. This author uses Fröman's "F-Matrix" formalism to obtain J.W.K.B. approximated wave functions on both sides of the coinciding classical turning points. It provides a very satisfactory expression for the penetrability at an incident energy close to the top of Strutinsky's barrier.

Recently, J.D. Cramer and J.R. Nix[45] claimed to have found an "exact" method of determining penetrabilities through two-peaked fission barriers. The exactness of the method is open to question in the light of various assumptions made by them for the sake of mathematical convenience, thus introducing approximation in regard to the physical situation. To make the physical picture more realistic, the author uses a new approximation called by him "Sharp Drop Approximation" and calculates the penetrability in Chapter V by a method similar to Cramer and Nix's. A cumbersome expression is obtained in terms of Weber parabolic cylinder functions.

Discussion of the J.W.K.B. results is given in Chapter VI. A justification of the "Sharp Drop Approximation" and a discussion of the results henceforth obtained is undertaken in the same Chapter. The conclusions drawn from the methods used and the results obtained are also reported in Chapter VI.

CHAPTER I

NUCLEAR FISSION

CHAPTER I

NUCLEAR FISSION

1.1 THE FISSION PROCESS

O. Hahn and F. Strasseman [1] discovered that alkaline earth metals are produced when Uranium is irradiated with neutrons. L. Meitner and O.R. Frisch [2] suggested that by absorption of neutrons, a Uranium nucleus becomes sufficiently excited to split into two fragments of approximately equal masses. This type of new reaction was called "fission" by Meitner and Frisch. [2]

That such a process is energetically possible can easily be seen from a study of atomic masses or binding energies of Uranium nuclei. The average binding energy per particle in the intermediate mass region ($A \sim 120$) is 8.5 Mev; in the Uranium region, however, it is only 7.6 Mev. If a heavy nucleus is split into two fragments, the increased binding energy per particle will be released in the form of kinetic energy of the fragments and through various types of radiations. From the above considerations, the total energy released in a fission process should be approximately

$$240\,(8.5 - 7.6) = 220 \text{ Mev} \qquad (1.1)$$

Since heavier nuclei are richer in neutrons than intermediate mass nuclei, two or three neutrons are released in

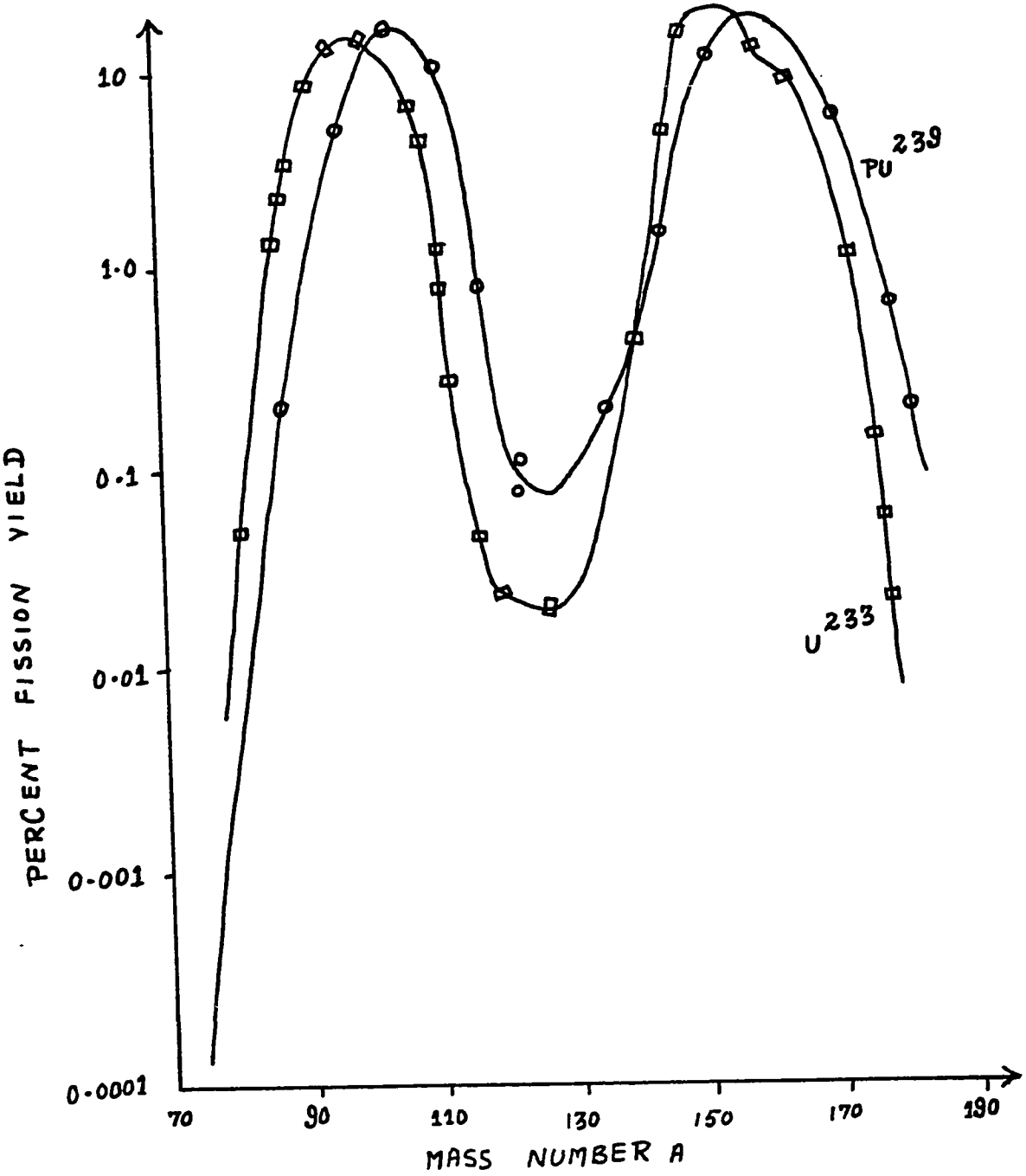

FIG. 1.1 Per Cent Fission Yield Versus A for U^{233} and Pu^{239}

every fission process at the expense of reaction energy, and after allowing for this loss, it is found that about 200 Mev is released.

Whatever the nature of the target nucleus and the mode of excitations, the particular physionomy of fission reaction is the result of the following fundamental properties:

- energy release

The energy released in a fission reaction is ten to a hundred times that produced by most of the exothermic nuclear reactions.

- mass yield

The splitting of the nucleus into two fragments of approximately equal masses is not unique. When bombarded by thermal (slow) neutrons, U^{235} can be split in thirty different ways, giving about sixty distinct fission products. Each splitting has a certain probability of occurrence. Fig. 1.1 gives the percentage yield of U^{233} and Pu^{239}, when bombarded with thermal neutrons. The curves corresponding to other very heavy nuclei, such as U^{235}, U^{238} or Th^{232} in the case of fast neutrons, are very similar to Fig. 1.1. The minima are less pronounced in case of fast neutron bombardment but the number of species of fission products obtained is the same. [3]

- prompt neutron emission

Along with the two fragments, several prompt neutrons are emitted. For Uranium and the neighbouring elements the fission threshold energies are low enough so that prompt neutrons have a higher kinetic energy than the fission threshold energy: these neutrons are able to activate new fission reactions,thus causing a chain reaction.

Furthermore, Fig. 1.1 shows that asymmetric fission is more frequent than symmetric fission. This arises from a simple consideration of U^{235}, where the sum of the masses ($Cd^{118} + Cd^{113}$) is 2 Mev higher than the sum of the masses ($Ze^{100} + Te^{136}$) corresponding to one of the most frequent asymmetric fissions. In the same way the electrostatic repulsion between the two fragments is proportional to the product of their charge, hence favouring asymmetric fission.

San Tsiang et al [4] published the first study of ternary fission in 1947. At the same time, they suggested the possibility of fission into four fragments. The usual ternary fission phenomenon yields two heavy nuclei and a high energy alpha particle of 10 to 40 Mev range. It was verified that this alpha particle emerges from the target nucleus and thus constitutes a third fragment. In the case of U^{235}, ternary fission is 300 to 400 times less probable than usual binary fission. Splitting into four

fragments may occur at very high excitation energies.

Fission of an atomic nucleus can either be spontaneous or be induced by bombardment with a number of projectiles at high, moderate or low energies. Thermal neutrons, as well as fast neutrons can induce fission of heavy nuclei. Fission in elements above atomic number 90, has been produced by bombardment with protons, deuterons and alpha particles. In 1940, Flerov and Petrzhak [5] discovered that natural Uranium undergoes spontaneous fission. The first attempt to observe the effect had been made in 1939 by Libby [6], but the detection equipment used was not sensitive enough to uncover it. Spontaneous fission and the alpha-decay process often compete for the break-up of an atomic nucleus.

1.2 THE FISSION MECHANISM : THE LIQUID DROP MODEL

Meitner and Frisch[2] suggested that medium mass products might result from nuclear fission, in a process analogous to the division of a charged liquid drop. Bohr and Wheeler [7] gave an extensive treatment of such a fission process in 1939.

The forces operating between the neutrons and the protons in the nucleus are short range, charge independent, nucleon / nucleon forces and the Coulomb repulsive forces of the protons. The shape assumed by the nucleus represents a balance between the nuclear forces, idealized as a surface tension and the Coulomb repulsive forces. The

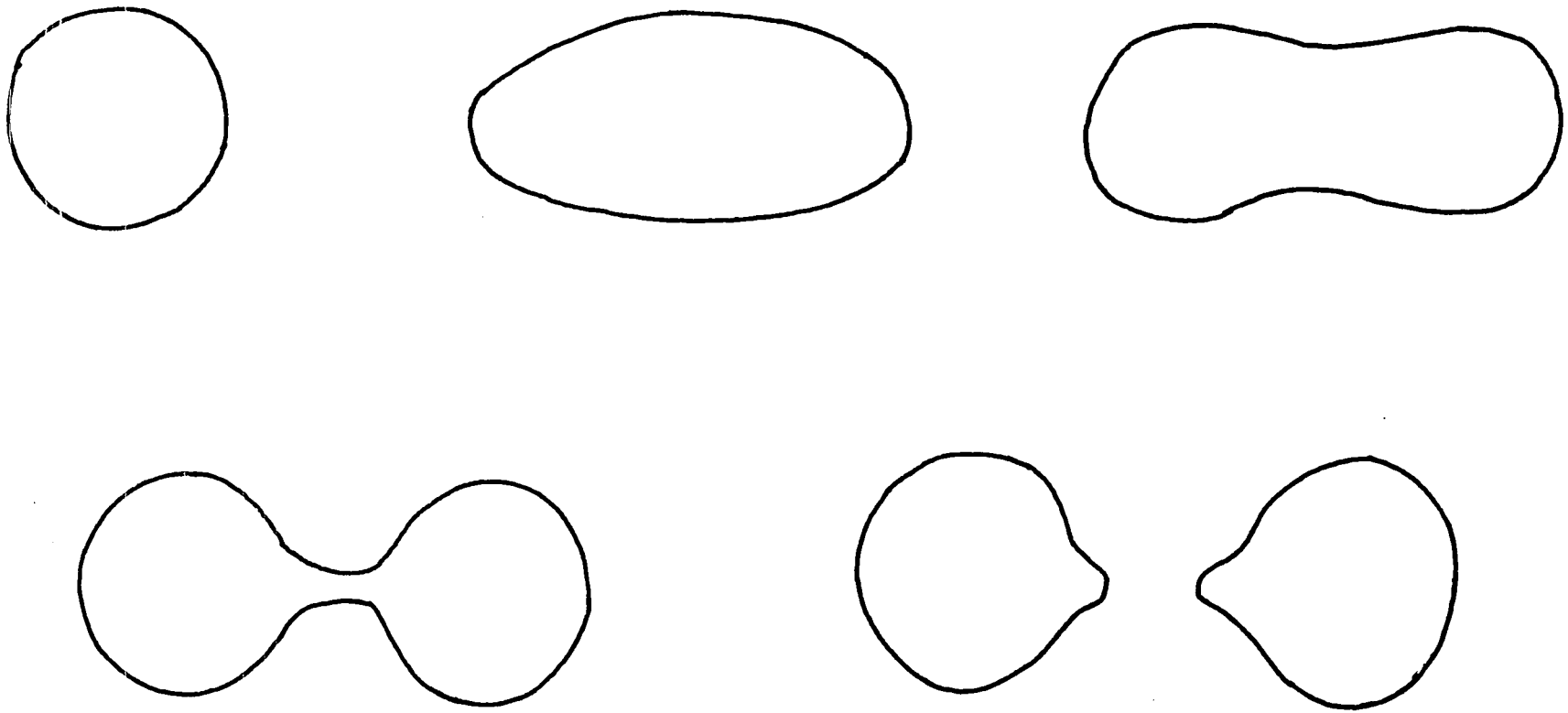

FIG. 1.2 The Fission Mechanism According to the Liquid Drop Model

strength of the surface tension can be estimated from the surface correction term in the semi-empirical mass equation while the strength of the Coulomb forces can be calculated from the proton charge, the proton number, the assumed volume distribution of protons within the nucleus and the dimensions of the nucleus. When excitation energy is added to the nucleus, oscillations are set up within the drop. This increases the surface area of the drop and the resultant increase in surface energy tends to return the drop to its original shape. If the electrostatic forces become greater than the surface tension, the deformation of the drop will grow and essentially the drop may divide into two or more fragments. Only the very heaviest elements have such a large protonic charge that relatively slight deformations of the nucleus can lead to fission. These qualitative considerations are illustrated in Fig. 1.2. The quantitative considerations are as given below.

1.2.1 The Liquid Drop Model : Statics

The statics of the Liquid Drop Model are best illustrated by an elementary calculation of the spontaneous fission limit and by potential energy surface mapping.

1.2.1.1 An Elementary Calculation of the Spontaneous Fission Limit on the Synthesis of Very Heavy Elements

A spherical nucleus is given a small symmetrical distortion of the $P_2(\cos\theta)$ type. The radius of the

slightly distorted sphere is given by

$$R(\theta) = R_0 \left[1 + \alpha_2 \; P_2 (\cos\theta)\right] \tag{1.2}$$

where $P_2(\cos\theta)$ is a legendre polynomial and α_2 a coefficient. It can be shown that

$$\begin{aligned} \text{surface energy} &= E_s = E_s^0 \left(1 + \tfrac{2}{5}\alpha_2^2 + \text{higher powers of } \alpha_2\right) \\ \text{electrostatic energy} &= E_c = E_c^0 \left(1 - \tfrac{1}{5}\alpha_2^2 + \text{higher powers of } \alpha_2\right) \end{aligned} \tag{1.3}$$

where E_s^0 and E_c^0 refer to the undistorted sphere. Hence the deformation energy is

$$\Delta V = V - V^{\text{SPHERE}} = \left(E_s - E_s^0\right) + \left(E_c - E_c^0\right) \tag{1.4}$$

$$= \tfrac{1}{5}\alpha_2^2 \left(2E_s^0 - E_c^0\right) + \text{higher powers of } \alpha_2 \tag{1.5}$$

For small distortions, higher powers of α_2 can be neglected and ΔV written

$$\Delta V = \tfrac{1}{5}\alpha_2^2 \left(2E_s^0 - E_c^0\right) \tag{1.6}$$

A spherical charged drop is then stable against small distortions of the $\alpha_2 P_2(\cos\theta)$ type if $2E_s^0 > E_c^0$ and unstable if $2E_s^0 < E_c^0$. If the charge is gradually increased on a liquid drop, then at a certain critical value of the charge corresponding to $E_c^0 = 2E_s^0$ (the saddle point shape), the drop will become unstable and divide spontaneously. For the case of an idealized nucleus, this is expressed differently in terms of a fissionability parameter x introduced by Bohr and Wheeler [7] and defined as follows:

$$x = \frac{E_c^\circ}{2E_s^\circ} \tag{1.7}$$

From electrostatics

$$E_c^\circ = \frac{3}{5}\frac{(Ze)^2}{R_0} \tag{1.8}$$

From an analysis of nuclear data, R_0 is found to be

$$R_0 = 1.216\ A^{\frac{1}{3}} \tag{1.9}$$

so that

$$E_c^\circ = \frac{0.713\ Z^2}{A^{\frac{1}{3}}} \tag{1.10}$$

From geometry

$$E_s^\circ = 4\pi R_0^2 \cdot \Omega \tag{1.11}$$

where Ω is the surface tension constant and is obtained from the semi-empirical mass formula. [8] Substituting (1.9) for R_0 and Ω by its value in Eqn. (1.11) yields

$$E_s^\circ = 17.80\ A^{\frac{2}{3}} \tag{1.12}$$

Therefore

$$x = \frac{E_c^\circ}{2E_s^\circ} = \frac{Z^2/A}{50.13} \tag{1.13}$$

The ratio $E_c^\circ/2E_s^\circ$ is proportional to the combination Z^2/A and

$$\left(\frac{Z^2}{A}\right)_{\text{CRITICAL}} = 50.13 \tag{1.14}$$

Eqn. (1.13) suggests that all nucleii of $Z \geq 120$ will be characterized by the absence of a classical barrier towards spontaneous fission.

1.2.1.2 Mapping of the Potential Energy Surface

These simple considerations on the stability of a spherical drop against small distortions of the $\alpha_2 P_2(\cos\theta)$ type must be replaced by much more complex calculations when larger distortions are considered, particularly when χ is substantially less than 1.0.

For distortions which are not too different from a sphere or spheroid, it is convenient to express the drop shape by the following radial equation:

$$R(\theta) = \frac{R_0}{\lambda}\left[1 + \sum_{n=1} \alpha_n P_n(\cos\theta)\right] \qquad (1.15)$$

where R_0 is the radius of the undistorted sphere, P_n is the legendre polynomial of order n and λ is a scale factor required by the condition of constant volume.

The task then is to map $V(\alpha)$ or ΔV in the many dimensional space of the α_n. For example, V or ΔV may be shown as contour lines on an $\alpha_2 - \alpha_4$ plot, which is the most important for small distortions of the symmetric type. Fig. 1.3 is an example of such a mapping.

The potential energy valleys are separated from one another and from the hollow around the spherical configuration by

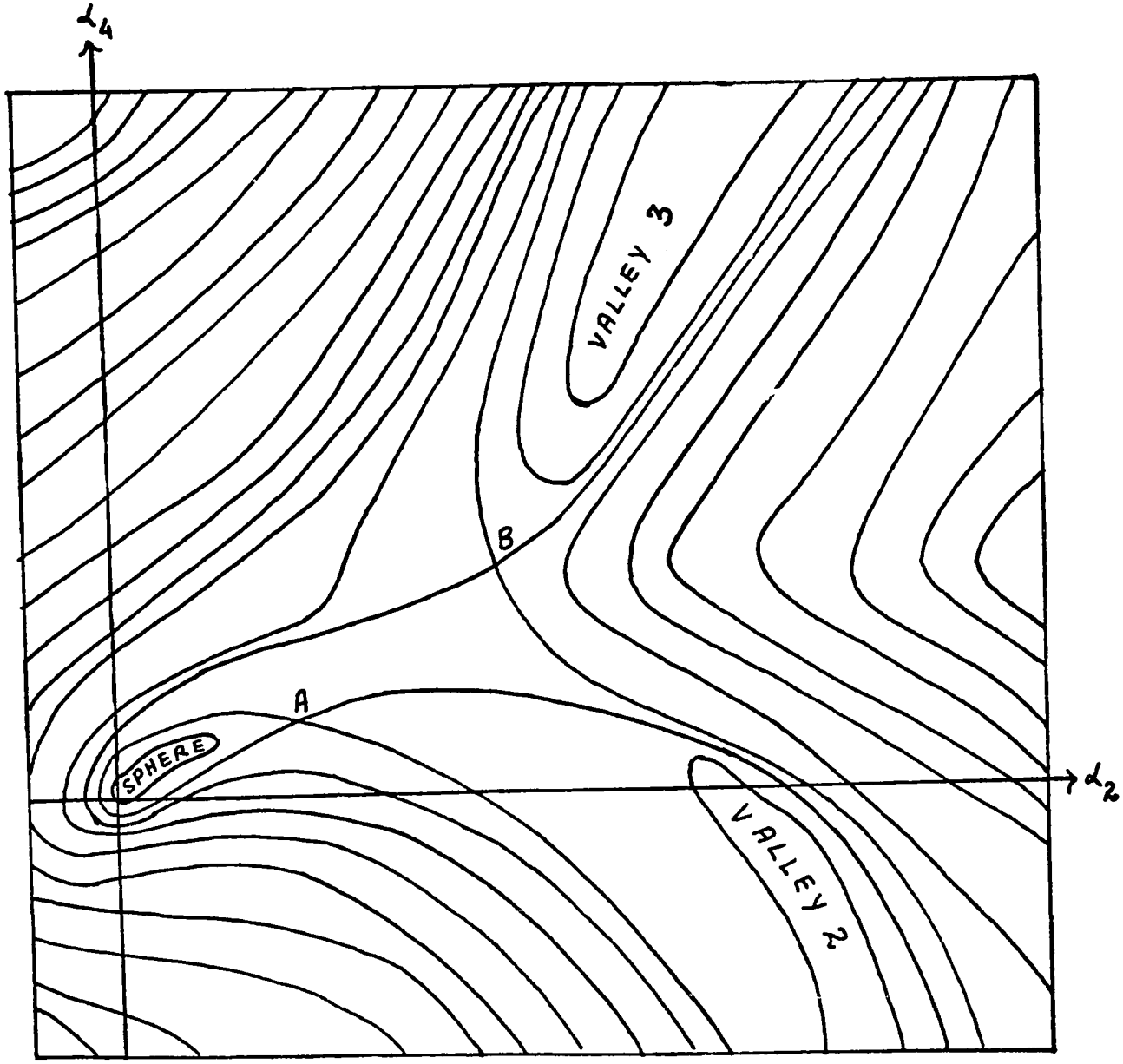

FIG. 1.3 Schematic α_2-α_4 Plot of Several Potential Energy Valleys

saddle points A and B. The reason for the name "saddle point" is that the potential energy surface has the appearance of a saddle or mountain pass. Point A lying lowest is the binary fission saddle point and point B, higher on the diagram, is the ternary fission one. [9] The potential energy surface maps are then important because they indicate the Liquid Drop Model saddle points.

1.2.2 The Liquid Drop Model: Dynamics

Since an ensemble of fissionable nuclei will actually exist in a great variety of initial conditions, a comprehensive calculation of the dynamics of such an ensemble would be a formidable task. Statistical mechanics can however, provide some notion about the average result of a large number of divisions.

The fission barrier depicted in Fig. 1.4 is the basis for a quantum-statistical-mechanical formulation of the fission mechanism in the Liquid Drop Model approximation. The height of the barrier corresponds to the saddle point energy. The tunneling through the barrier is responsible for spontaneous fission. Bohr and Wheeler [8] obtained a fission rate from such a barrier. Obviously the fission rate decreases as the energy is lowered from its saddle point value. On the other hand, Hill and Wheeler [10] calculated the penetrability of such a potential barrier and from those calculations obtained the half-lives of the corresponding nuclides. The height and shape of the barrier

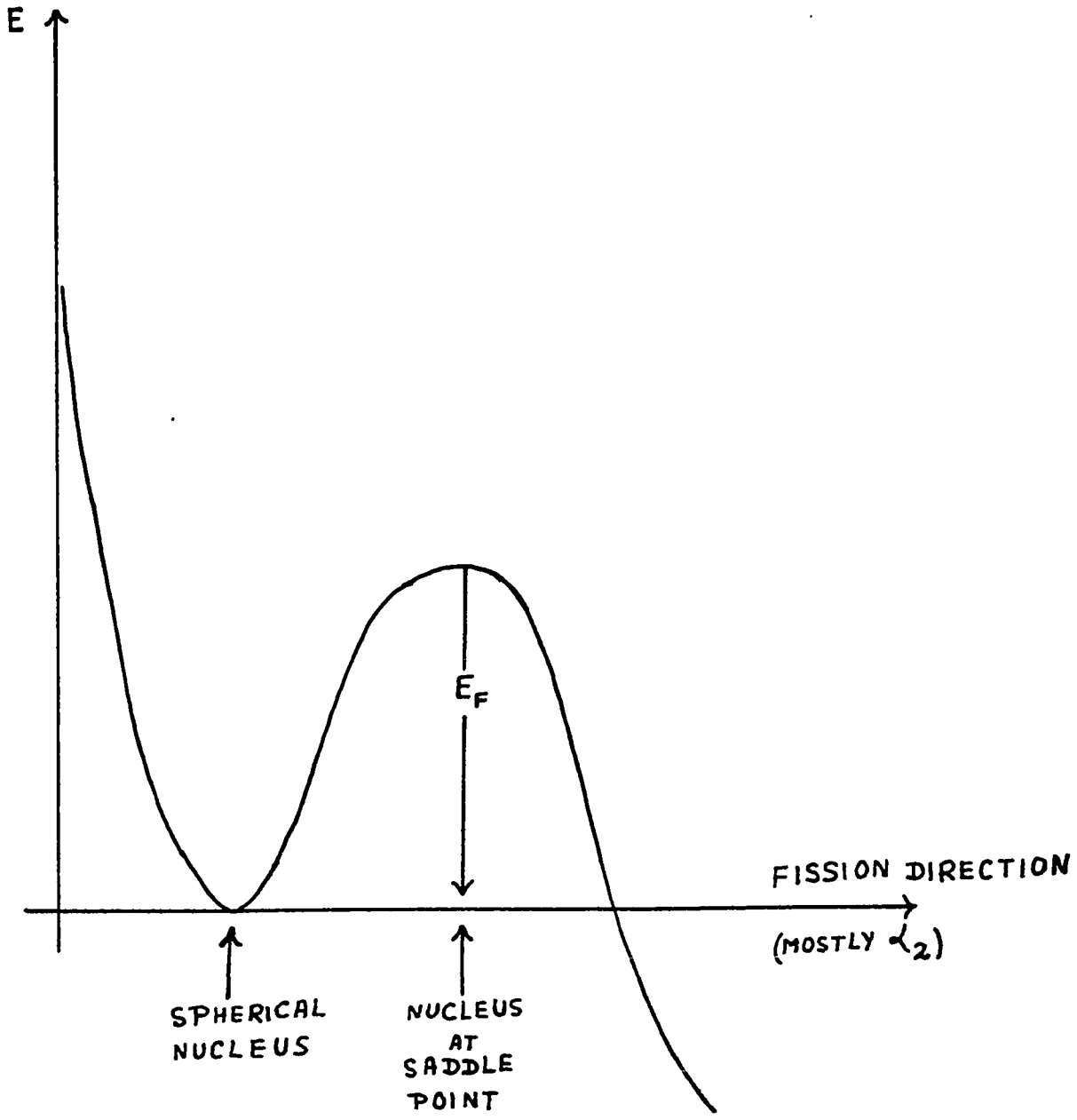

FIG. 1.4 Bohr and Wheeler's Fission Barrier

will vary from one nucleus to the next.

1.3 THE FISSION MECHANISM : THE COLLECTIVE MODEL

Following the Liquid Drop Model, the next major advance in sophistication is the introduction of particle degrees of freedom. In fact, the Liquid Drop Model and the Independent Particle Model grew up separately and in many ways appear to be incompatible. The Unified Models of Rainwater,[11] Bohr and Mottelson,[12] Hill and Wheeler [10] incorporated features of both models by the simultaneous introduction of collective and independent particle coordinates.

1.3.1 The Collective Model in the Region of Deformed Nuclei

The Collective Model description of deformed or strongly deformed nuclei is of prime importance for the fission process. At some considerable distance from closed shells, the nucleus becomes stabilized in a non-spherical shape under the influence of the coherent effects of many particles in unfilled shells. The adiabatic approximation holds and the wave function describing the nucleus as a whole can be separated as follows:

$$\Psi = \chi_{PART} \cdot \phi_{VIB} \cdot D_{ROT} \qquad (1.16)$$

χ_{PART} describes the intrinsic motion of the nucleus expressed in terms of the independent motion of the individual

particles in the deformed field. Quantitatively χ_{part} is Nilsson's Model [13] wave function. ϕ_{vib} depicts the vibrations of the nucleus around its equilibrium shape. D_{rot} identifies with the rotational motion of the system as a whole.

The coupling scheme [12] for deformed nuclei is defined by Fig. 1.5. The three important constants of the motion are I, K and M where I is the total angular momentum of the nucleus, K is the projection of I on the axis of symmetry and M the projection of I on a space fixed axis z. For the ground state and for low lying excited states in which there is no collective rotation about z', the body fixed axis, K is taken equal to Ω' which is defined as the projection of the total particle angular momentum on the nuclear symmetry axis. The total angular momentum $\sum_i j_i$ of the particle system is not, in general, a constant of the motion. K will be different from Ω' for certain types of vibrational excitations in which collective angular momentum is contributed along the nucleus axis.

1.3.2 Nuclear Fission and the Collective Model

1.3.2.1 Special Role of the Saddle Point

The saddle point configuration plays a special role in the fission process. [14] Since the amount of energy tied up in the deformation is greatest here, the collective motion is also slowest and the adiabatic approximation is

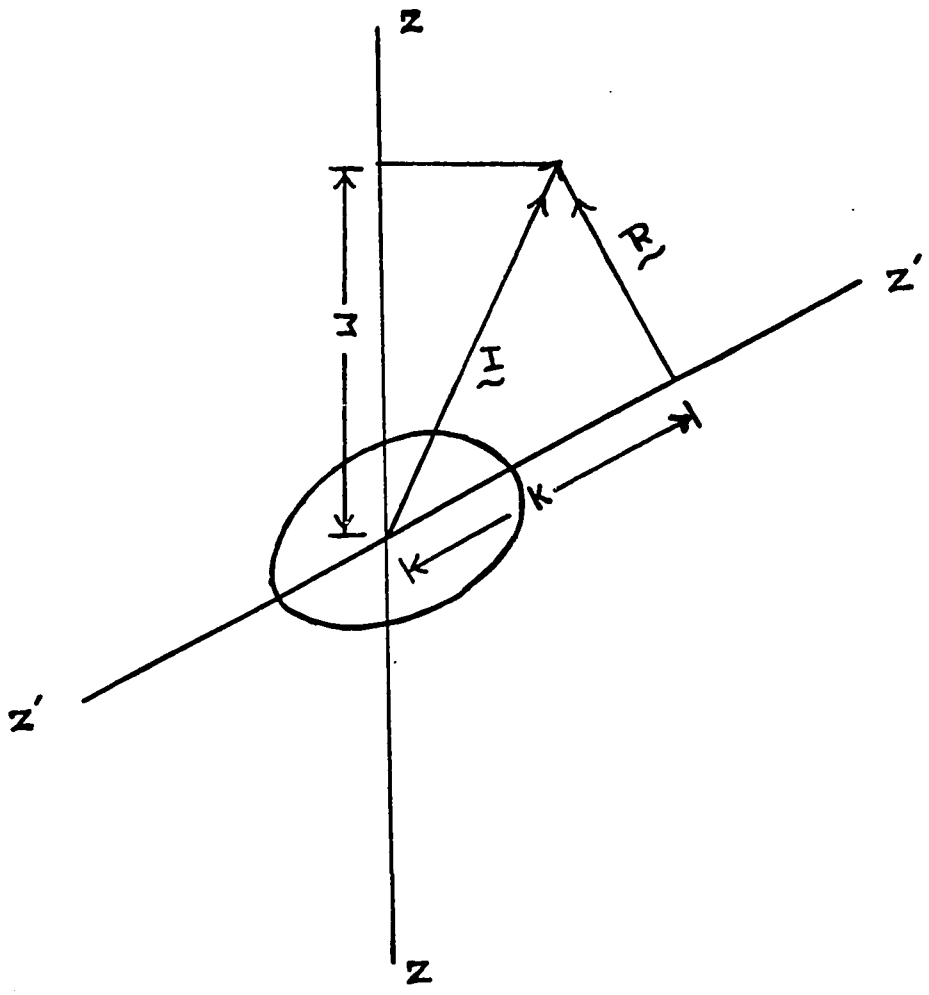

FIG. 1.5 The Coupling Scheme for Deformed Nuclei

valid here. The saddle point is a bottleneck for the fission process : the system must pass through (or near to) it with minimum energy available for collective dynamics and intrinsic excitations. It is at the saddle point that constants of the motion are frozen into the system. It seems plausible that along the dynamical path from the saddle point to scission (the rupture into 2,3 or n fragments), the deformation maintains an axial symmetry which preserves Ω' as a constant of the motion. The goodness of Ω' is well established for strongly deformed ground state nuclei (Nuclear surface energy and pairing correlation tend to favour axial symmetry just as they also favour spherical symmetry).[15] Even if the adiabatic approximation breaks down beyond the saddle point, the constancy of Ω' should be preserved.

1.3.2.2 Spontaneous Fission Lifetime

The Collective Model indicates that the potential barrier for odd-A nuclei is greater than for even-even nuclei. Spontaneous fission lifetimes will then be higher for even-even nuclei, in agreement with experiment.

1.3.2.3 Angular Distribution of Fission Fragments

The angular distribution of fission fragments is completely determined by the relative "orbital" angular momentum vector $\underset{\sim}{R}$ of the fragments as defined in Fig. 1.6. To the extent that Ω', the projected angular momentum along the z' axis, is a constant of the motion at scission, the

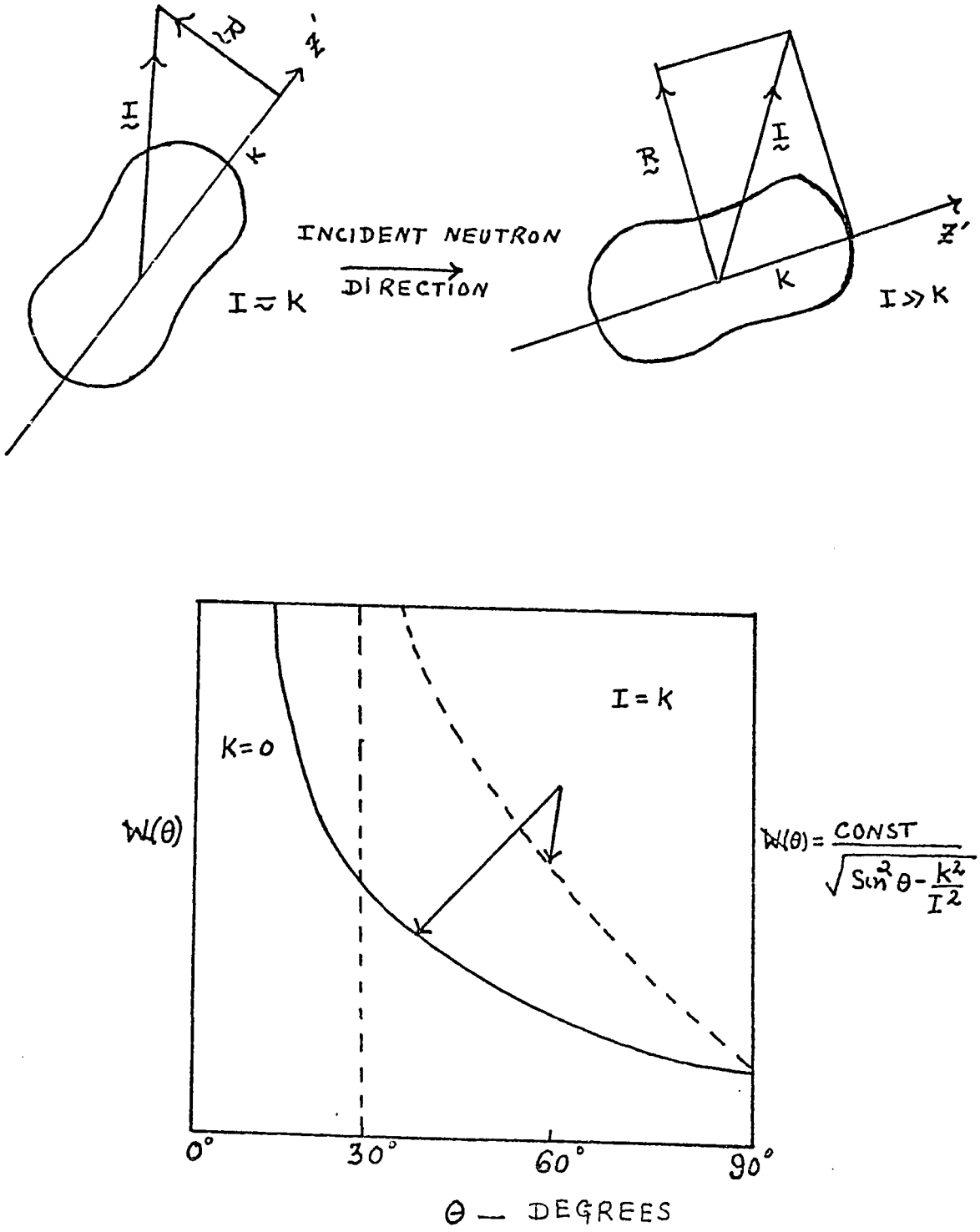

FIG. 1.6 Classified Vector Model for the Angular Distribution of Fission Fragments

total angular momentum of the system is given by

$$\underset{\sim}{I} = \underset{\sim}{R} + \underset{\sim}{\Omega'} \qquad (1.17)$$

which is, of course, a rigorous constant of the motion. $\underset{\sim}{I}$ is determined by the condition of formation of the compound system. For example, a neutron is incident upon an even-even target. The classical angular momentum considerations, neglecting neutron spin are depicted in Fig. 1.6. The angular momentum vector of the neutron, and hence also of the compound system, points normal to the incident direction. The vectors $\underset{\sim}{R}$ and $\underset{\sim}{\Omega'}$ precess about $\underset{\sim}{I}$ and $\underset{\sim}{I}$ must be averaged over all directions normal to the incident direction. Thus the final angular distribution of fragments is the distribution in the direction of the symmetry axis $\underset{\sim}{z'} = \underset{\sim}{\Omega'}$, as obtained by executing the above averages. The classical angular distributions of fission fragments for unique values of I and Ω', as first given by Bohr, [16] are

$$W^{I}_{\Omega'}(\theta) \propto \sin^2\theta - \frac{\Omega'^2}{I^2} \qquad (1.18)$$

They are also displayed in Fig. 1.6. The correct quantum mechanical expression for unique I and Ω, but with unpolarized projectile momentum Λ is

$$W^{I}_{\Omega'}(\theta) \propto \sum_{M,-\Lambda}^{+\Lambda} \left| D^{I}_{M\Omega'} \right|^2 \qquad (1.19)$$

1.3.2.4 Mass Yield

Ever since the observations of M. Mayer [17] that mass asymmetry was correlated with nuclear shell structure, there have been efforts to insert this information into the fission mechanism . The problem is to know to what extent shell effects do persist at moderate and large deformations where degeneracies could be effectively removed. A hint that shell effects do persist comes from the observed odd-parity (1^-,3^-,5^-) excitations of even-even nuclei. It is proposed that they are members of the ground state rotational band, but correspond to the first octupole vibrational excitations. Inglis [15] pointed out that the 136 neutrons of Ra^{136} - which has the lowest 1^- state - could be interpreted as being grouped asymmetrically into stable structures of 50 and 82 neutrons, joined by a neck of four neutrons. Protons, of course, are also present. A. Bohr [16] proposed that for fission resulting from slow neutron capture, the mass yield should vary from resonance to resonance or from resonance to off-resonance. Experimental investigations have revealed resonance structure in the mass asymmetry; the effect is not as drastic as the theory might imply. [19]

1.4 THE NEED FOR OTHER MODELS

The problem of nuclear masses and their dependence on deformation has to be resolved if there is to be hope of a consistent and widely applicable fission formalism. There are several approaches to the problem, one of which is the

Liquid Drop Model. This model however, ignores completely nucleon shell effects. The importance of such quantum effects is stressed however, in the Bohr-Mottelson unified model,[12] but the model still offers only a qualitative picture of the consequence of these effects for the fission process. In more microscopic models, an attempt is made to reduce the problem of nuclear masses and deformation energies to residual nucleon interactions.

A completely quantitative microscopic description of nuclear deformation and fission is hardly possible at the moment. Modern theories of nuclear excitations use a renormalized Hamiltonian and assume that the properties of the average field are known from empirical data. The problem of nuclear masses and deformation energies is complicated by the necessity of calculating the average field and the energy related to it and some other quantities such as the surface tension constant. In the surface region the nuclear density decreases to zero in a very short distance of the order of $A^{-\frac{1}{3}} R_0$, i.e. a large density gradient is present. The problem of surface tension arises for which features of nuclear interactions such as saturation (velocity dependence) are important. In fact,there are relatively simple ways to account for these surface effects in classical phenomenological models. These can be taken from some known general features of nuclei, in particular from average data on nuclear masses. They are not influenced sensibly by shells.

A method of including shells and other quantum effects in nuclear masses and deformation energies has been devised recently : Strutinsky's Shell Correction Method.

CHAPTER II

THE DOUBLE HUMP FISSION BARRIER

CHAPTER II

THE DOUBLE HUMP FISSION BARRIER

2.1 THE SHELL CORRECTION METHOD

2.1.1 Main Features of the Method

Strutinsky [20] considers nucleon shells and other quantum effects as a small deviation from a uniform distribution and the corresponding correction to the Liquid Drop Model energy is then determined. When the difference of the two distributions becomes small, the energy difference will be a linear combination of the difference between the two nucleon distributions. Furthermore, the energy difference (with an accuracy up to the residual interaction) may be expressed simply as a difference of the single particle energies

$$\delta U = U - \tilde{U} \tag{2.1}$$

of the shell quantal distribution of nucleons

$$U = \sum_{\nu} E_{\nu}\, 2 n_{\nu} \tag{2.2}$$

with the sum over all occupied states and the uniform distribution

$$\tilde{U} = 2 \int_{-\infty}^{\tilde{\lambda}} E\, \tilde{g}(E)\, dE \tag{2.3}$$

A tilda above the letter indicates quantities for the uniform distribution, and the same letter without a tilda refers to the analogous quantity for the quantal distribution

of nucleons. In Eqn. (2.2), E_ν are nucleon levels in the average potential and n_ν the occupation numbers. In Eqn. (2.3), $\tilde{g}(\varepsilon)$ is a uniform distribution of nucleon states and the quantity $\tilde{\lambda}$ is the Fermi energy which is determined from the conservation of the particle number.

It is assumed that the shell model average potential well is a self-consistent potential for the uniform distribution. A realistic distribution of nucleons could be a Nilsson potential level scheme [13] or a Woods-Saxon level scheme. [21] The residual interaction effects are also influenced by shells and will be included in the total energy. This total energy is written as a sum of the Liquid Drop Model energy W_l, the residual interaction and the shell correction

$$W_l = \tilde{W}_l + \sum_{p,n} (\delta U + P) \qquad (2.4)$$

The sum is over protons and neutrons. Of the residual interactions, the most important one is the nuclear pairing energy, because of its strong exponential dependence on the density of nucleon states. The pairing energy can be calculated in the usual approximation of the B.C.S. Theory. The shell correction δP to the pairing energy is the difference between P and the pairing energy $\tilde{P}$ calculated for the uniform distribution of single particle states.

Strutinsky's development of the shell correction method suggests that shells can be considered more generally

as non-uniformities in the energy distribution of nucleons near the Fermi surfaces. [20] In fact, when a nucleus is deformed, a compression of the single particle nucleon levels near the Fermi energy alternates with a thinning out or a shell and this leads to modulations in the Liquid Drop Model (L.D.M.) energy of the nucleus.

2.1.2 Consequences of the Shell Correction Method

Strutinsky [22] shows that, contrary to existing opinion, the shell non-uniformities in the energy distribution of the nucleons do not disappear in deformed and strongly deformed nuclei.

He also points out that the shell correction method ascribes equivalent effects to particle numbers and deformations. [25] With the former variable, the measured nucleidic masses provide a rich basis for the study of deviations from the average and for comparison with calculations based on realistic single particle energy diagrams. This is illustrated in Fig. 2.1. In Fig. 2.1, there is agreement in considerable detail. The effect of the other variable, i.e. deformation, gives rise to an unexpected behaviour of nuclear deformation energies with respect to the prolate deformation coordinate β. This forms the basis for Strutinsky's model of fission.

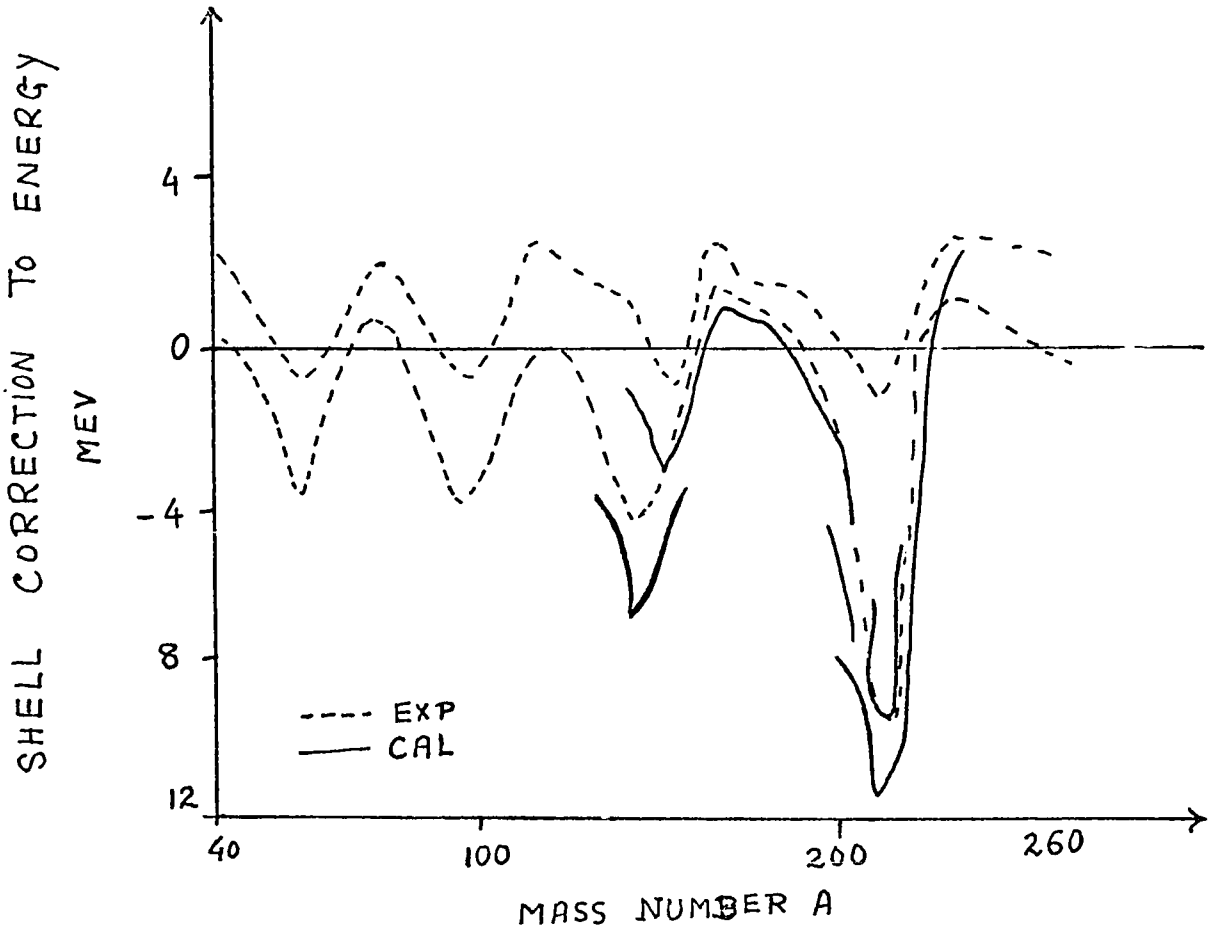

FIG. 2.1 Corrections to Ground State Masses Due to Shell Effects (Heavy Lines) Compared With Experimentally Observed Deviation From a Best Fit Liquid Drop Model Mass

2.2 STRUTINSKY'S MODEL OF FISSION : THE DOUBLE HUMP BARRIER

2.2.1 The Shell Correction Method and Nuclear Fission

For very heavy nuclei the surface tension constant in L.D.M. is very small or even negative. However, the known fission barriers and spontaneous fission lifetimes do not decrease very fast and the experimental nuclear deformations do not decrease in this region. This anomaly is explained by Strutinsky [24] on the basis of the shell corrections to nuclear deformation energies.

Some results of the calculations for the heaviest nuclei are shown in Fig. 2.2. The first minimum of the potential energy corresponds to a ground state which turns out to be a few Mev lower than the spherical energy in L.D.M. This is an effect of the deformed state shell $N\sim150$, which is essential for equilibrium deformations in this region. The stiffness of the nuclear shape in the ground state is also determined by this shell. The stiffness and equilibrium deformations do not change much in this region, in spite of a sharp decrease of the effective surface tension in L.D.M. Energetically the shell effects are most pronounced in Cp , but their influence extends over a broad region of nuclei. The $N\sim150$ shell is very important for the stability of the transuranic elements against fission. Strong shells appear again in still heavier "magic number" nuclei for the

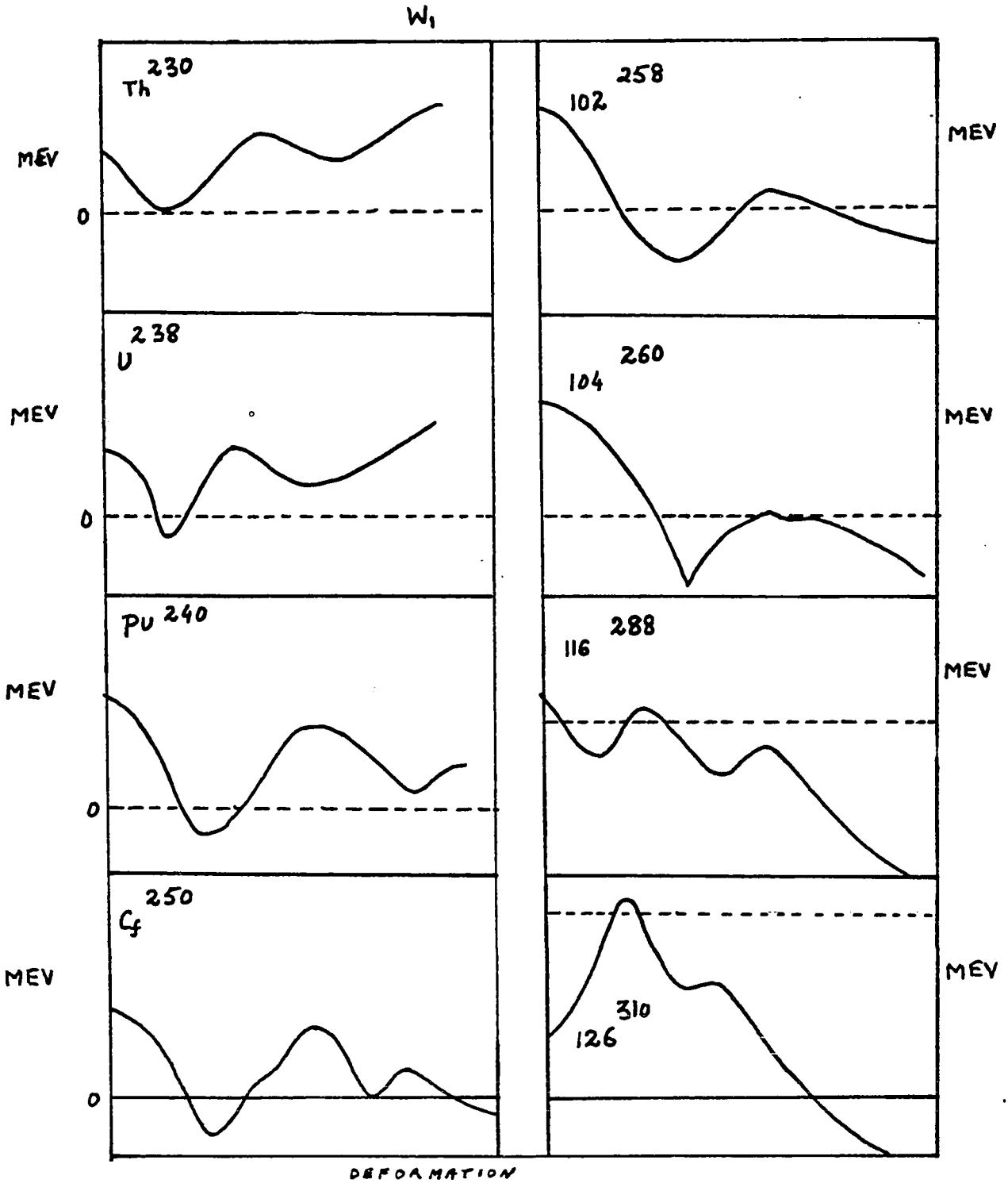

FIG. 2.2 Nuclear Deformation Energy W_1 For Heavy and Super Heavy Nuclei

spherical shape. As a result these nuclei are relatively more stable against fission as was already suggested by Swiatecki.[25] The fission thresholds of deformed transuranic nuclei turn out to be larger than the ones in L.D.M. and they do not depend much on Z^2/A. It should be noticed, however, that due to a second minimum of the shell correction, the saddle point is strongly deformed in these calculations and there are in fact, two or even three fission barriers in Fig. 2.2, as a well pronounced minimum appears near the saddle point in nuclei from Th to Cf. This minimum corresponds to deformation about twice that of the ground state and is due to the crossing of the levels of the shells next to one corresponding to the Fermi energy.

2.2.2 Strutinsky's Model of Fission

Strutinsky [24] set the basis of his model in 1968, after careful study of the above results. The L.D.M. potential is retained and corrections to nuclear masses and deformation energies as given by the L.D.M. are calculated by the Shell Correction Method. The single particle states of the deformed potential are included in the model through the Shell Correction Method. The distribution of nucleons is taken as in the Nilsson potential level scheme [13] or in a Woods-Saxon potential level scheme. [21]

Strutinsky's model is therefore a collective model. The adiabatic approximation is still valid as the collective excitation period is much greater than the

particle motion period. The model calculations yield a double hump fission barrier. [26] This two-peaked fission barrier, although hinted at by Swiatecki,[25] is a radically new feature in the fission formalism. A schematic diagram representing the barrier is given by Fig. 2.3. As said before, in all nuclei where the double hump fission barrier applies, the second minimum occurs at a deformation about twice that of the ground state. Only prolate deformations have been considered in the calculations. This model best applies for heavy nuclei with neutron numbers in the vicinity of 146-148, i.e., in the Actinides region. It is to be noted that the fission barrier of Fig. 2.3 is somewhat dependent on the single particle model used. [26] The existence of two minima separated by an internal energy barrier means that the excitations of the nucleus can be divided into two classes. The states of the first well are denoted by Class I states and those of the second well as Class II states. These Class I and Class II states are also represented in Fig. 2.3. A wealth of new consequences follows from the weak coupling between the degrees of freedom associated with each of the two wells.

2.2.3 Theoretical Implication of Strutinsky's Model

2.2.3.1 Two Intermediate States in a Hot Compound Nucleus

In hot nuclei, a fast dissipation of the collective motion normally takes place and, as a result, the nucleus

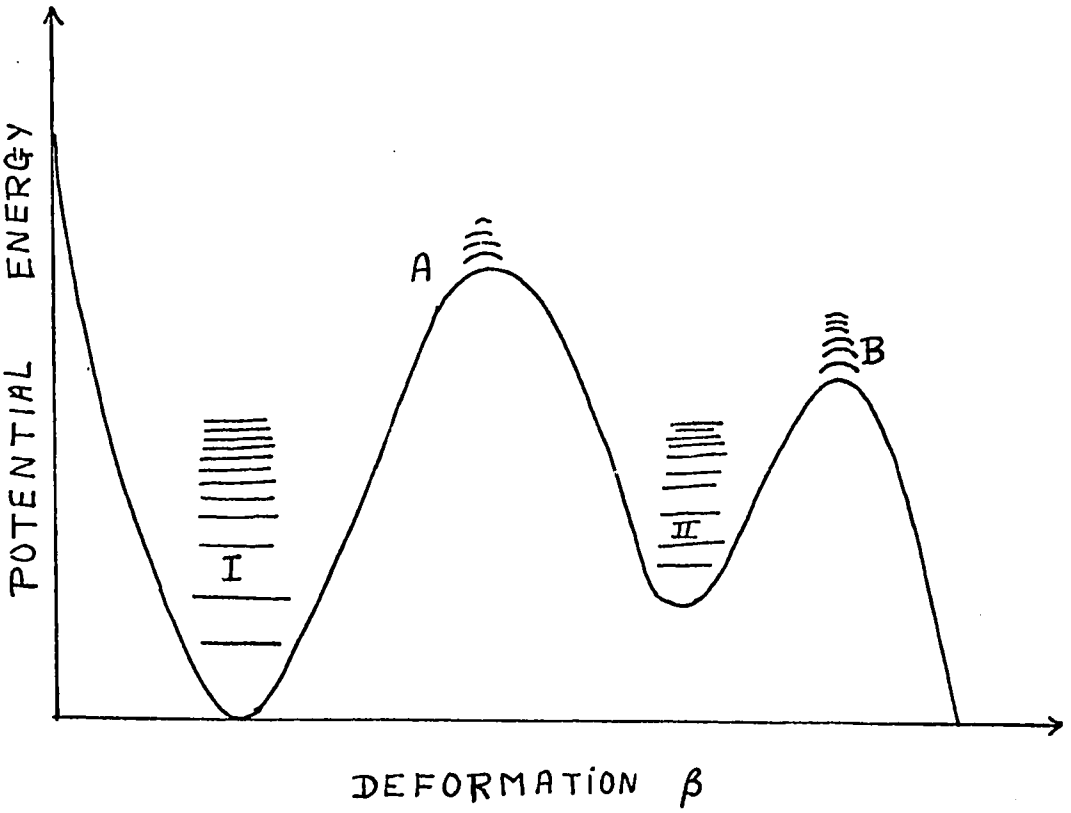

FIG. 2.3 Strutinsky's Fission Barrier. The Intrinsic Excitations Are Shown

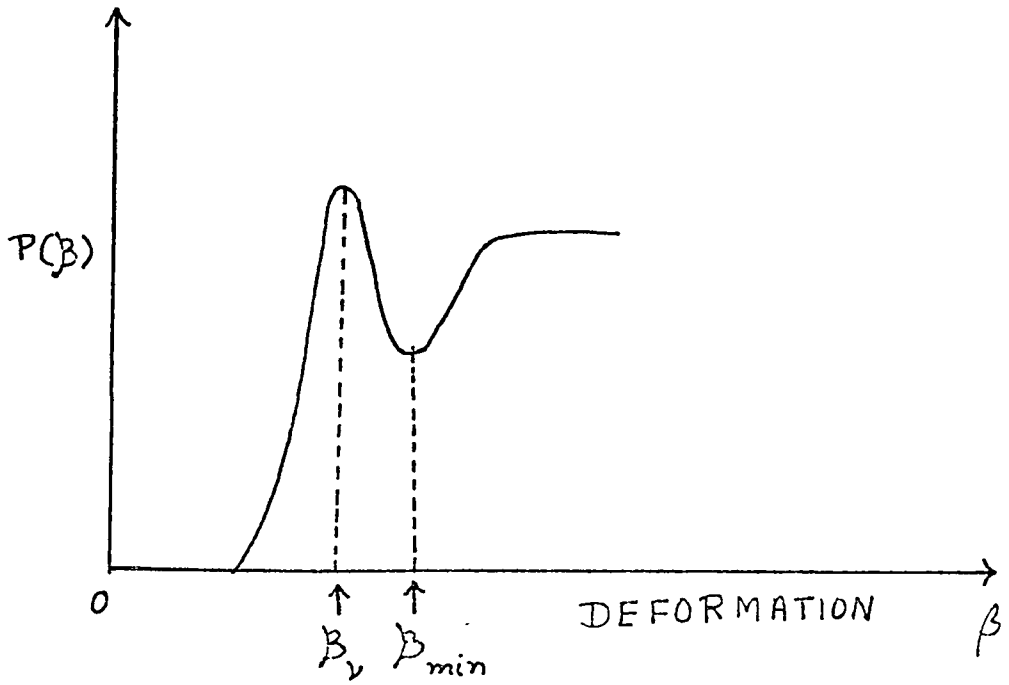

FIG. 2.4 Penetration Function of Strutinsky's Fission Barrier for Vibrational Motion in The Fission Direction

takes a shape corresponding to one or the other of the two energy minima. In the collective, as well as in each of the one particle degrees of freedom, a relatively small amount of energy of the order of the nuclear temperature T is collected. If T is smaller than the depth of the potential well, the nucleus maintains its equilibrium shape for a relatively long time. Thus, there are two intermediate states of the compound nucleus, each with its own temperature, spectrum, etc. For reactions produced by monochromatic neutrons one may expect structures related to the states in the second potential well; particularly in the distribution of fission resonances, the fission width must be especially large, with capture resonances which are close in energy to these states. The fission cross-section is modulated by this structure and the energy width of these modulations correspond to the spreading width of the quasi-equilibrium states in the second well. [27]

2.2.3.2 Vibration Mode Resonances

The resonances described in Section 2.2.3.1 correspond to many-particle states of the compound nucleus. In principle, there can be also a resonance structure related to the vibrational states in the fission degree of freedom. A new possibility arises in the two-well model. Here, some of the vibrational states correspond to wave functions in the second well. The nucleus is cold if the bottom of the second well is several Mev above the first one. For the vibrational states, the conditions for vibrational mode resonances can be

fulfilled if a collective vibrational level at energy around 5 Mev is the first or second excited state, or perhaps even the ground state level in the second potential well. The width of such a low lying state will be determined by the penetrability through the potential barrier and by the purity of the collective states in the second well, i.e., the degree of damping. In vibrational mode resonances, the penetrability attains a maximum value at resonance energy β_γ, as depicted in Fig. 2.4.

2.2.3.3 Angular Distribution of Fission Fragments

Another consequence of a two-humped barrier is its effect on the angular distribution of fission fragments. The nucleus may forget its orientation because it stays in the second well for a time long enough for Coriolis forces to redistribute the angular momentum projection with which the nucleus passed through the first barrier. The second barrier gives rise to channel structure in anisotropies in the angular distribution of fission fragments if the second well is deep enough. Now, if the second barrier lies lower than the first, many channels will be open and a weak, statistical type, angular anisotropy will result even in the near-barrier (i.e. near the barrier B) fission. This is important because in the usual picture of channel effects, the channel structure must invariably be present near the barrier.

2.2.3.4 Shape Isomerism

The spectrum of excited states in the second well gives rise to intermediate structure effects. The ground state of the spectrum will manifest itself as an isomer decaying either by barrier penetration or by beta or alpha-decay. [28] The double-humped potential makes spontaneously fissioning isomers more likely. An isomer decaying by barrier penetration is said to be a shape isomer.

2.3 SUCCESS OF THE MODEL

The existence of the double hump fission barrier with a secondary minimum in between the peaks is strongly supported by the discovery of fission isomers (also called shape isomers). Experimentally these isomeric states are found to decay by spontaneous fission rather than γ-emission. The first fission isomer in Am^{242}, discovered by Polikanov et al [29] and by Flerov et al, [30] has a fission half-life of 14 ms. Since then a number of other cases have been found with half-lives ranging from nanoseconds to milliseconds. [31] The isotope of Am^{242} seems to have an unusually long fission half-life.

Evidence in support of vibrational mode resonances in the fission cross-section was collected by Vorotnikov et al [32] in the reaction ($Th^{230} + n$). The experimental results are reproduced in Fig. 2.5. A pronounced maximum is found for energies below the barrier.

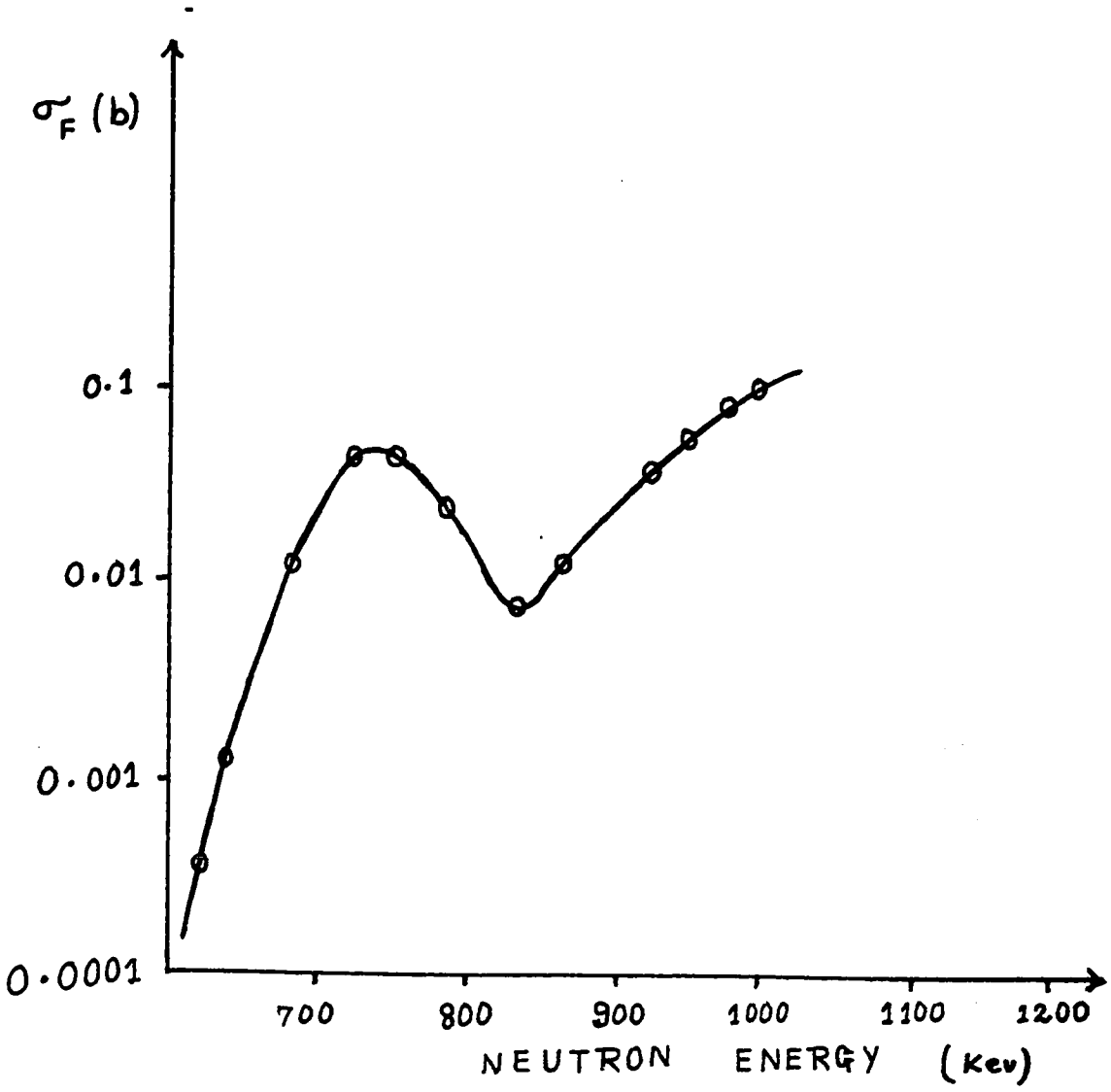

FIG. 2.5 The Fission Cross-Section $\sigma_F(b)$ of Th^{230} With Neutrons

Only vibrational mode resonance can explain a maximum in this energy range. Very interesting results were obtained by Kapitza et al [33] in studies of photofission cross-sections and angular distribution of fission fragments for five even nuclides. Again, structures appear here which cannot be explained in terms of a single barrier. These structures tend to indicate vibrational type resonances.

Strutinsky's model relates angular anisotropies of fragments in the heaviest nuclei with a distribution of K values over the second barrier. In the reaction ($Am^{241} + n$), the observed anistropy is about 7% for 1.0 - 2.0 Mev excitation energy above the barrier and is in reasonable agreement with theory.

Furthermore, Androsenko and Smirenkin [34] found that for fission of U^{238} near the barrier, the distribution of K (the projection of the angular momentum vector) showed a lack of structure, thus supporting Strutinsky's hypothesis that the second minimum makes the absence of structure possible.

Theoretically, the presence of a second minimum is rather a general feature in the sense that it is obtained in all realistic models known at present, including the finite depth Woods-Saxon Model. [35] It is also found to be stable against γ_4 deformations, [36] the non-axially symmetric γ - deformations (oblate deformations) [37] and the octupole deformations.

CHAPTER III

THE J.W.K.B. APPROXIMATION

CHAPTER III

THE J.W.K.B. APPROXIMATION

For Strutinsky's fission barrier it is best to use the J.W.K.B. approximation to calculate penetrabilities.

3.1 BOHM'S CONNECTION FORMULAE [38]

3.1.1 Barrier to the Right

Supposing $V > E$ to the right of a point $x = a$, and putting

$$\frac{\sqrt{2m(E-V)}}{\hbar} = \chi \tag{3.1}$$

$$\frac{\sqrt{2m(V-E)}}{\hbar} = k \tag{3.2}$$

far to the right of $x = a$, Bohm's approximate solution is a decaying exponential, namely:

$$\Psi = \frac{1}{\sqrt{\chi}} \exp\left(-\int_a^x \chi \, dx\right) \tag{3.3}$$

Far to the left of $x = a$, this solution approaches

$$\Psi = \frac{2}{\sqrt{k}} \cos\left(\int_x^a k \, dx - \pi/4\right) \tag{3.4}$$

Hence the connection formula

$$\frac{1}{\sqrt{\chi}} \exp\left(-\int_a^x \chi \, dx\right) \rightleftharpoons \frac{2}{\sqrt{k}} \cos\left(\int_x^a k \, dx - \pi/4\right) \tag{3.5}$$

Similarly it may be shown that the connection formula for solutions which approach an increasing exponential to the right of $x = a$ is

$$\frac{1}{\sqrt{k}} \sin\left(\int_x^a k\,dx - \pi/4\right) \leftrightharpoons -\frac{1}{\sqrt{\chi}} \exp\left(\int_a^x \chi\,dx\right) \qquad (3.6)$$

3.1.2 Barrier to the Left

It is convenient to write down the formulae in the case where the classically forbidden region is to the left of $x = a$. For the solution which decays exponentially to the left, the connection formula is

$$\frac{1}{\sqrt{\chi}} \exp\left(-\int_a^x \chi\,dx\right) \leftrightharpoons \frac{2}{\sqrt{k}} \cos\left(\int_a^x k\,dx - \pi/4\right) \qquad (3.7)$$

or, if the wave function increases exponentially to the left, the formula becomes

$$\frac{1}{\sqrt{k}} \sin\left(\int_a^x k\,dx - \pi/4\right) \leftrightharpoons -\frac{1}{\sqrt{\chi}} \exp\left(\int_x^a k\,dx\right) \qquad (3.8)$$

3.2 FRÖMAN'S "F-MATRIX" FORMALISM [39]

3.2.1 Fröman's J.W.K.B. Approximated Solution to a General Schrödinger Equation

Fröman considers the one-dimensional time independent Schrödinger equation

$$\frac{d^2\psi}{dz^2} + Q^2(z)\,\psi = 0 \qquad (3.9)$$

where η is a complex variable and $Q^2(\eta)$ is a function which is analytic and single valued in a certain region of the complex η-plane. He introduces instead of η and ψ the new variables ω and φ which are defined by

$$\left.\begin{aligned} \psi &= \left[q(\eta)^{\frac{1}{2}}\right]\varphi(\eta) \\ \omega(\eta) &= \int^{\eta} q(\xi)\, d\xi \end{aligned}\right\} \qquad (3.10)$$

The differential eqn. (3.9) then transforms to

$$\frac{d^2\varphi}{d\omega^2} + (1+\varepsilon)\,\varphi = 0 \qquad (3.11)$$

where ε is given by

$$\varepsilon = \frac{q^2 - q^2}{q^2} - q^{-\frac{1}{2}}\,\frac{d^2}{d\omega^2}\left(q^{\frac{1}{2}}\right) \qquad (3.12)$$

The functions $\exp(i\omega)$ and $\exp(-i\omega)$ are exact solutions of the differential eqn. (3.11) if $\varepsilon = 0$, i.e. if $q(\eta)$ satisfies the differential equation

$$q^2 - q^{\frac{1}{2}}\,\frac{d^2}{d\eta^2}\left(q^{-\frac{1}{2}}\right) = Q^2 \qquad (3.13)$$

Knowing any solutions $q(\eta)$ of this differential equation, one has the following two linearly independent, exact solutions of the differential eqn. (3.9)

$$\psi = q^{-\frac{1}{2}}\,\exp\left\{\pm i\int^{\eta} q(\xi)\, d\xi\right\} \qquad (3.14)$$

Fröman then cuts the complex ω-plane in such a way that the functions are all single valued and he expresses φ in the form

$$\varphi = a_1(w) \exp(i w) + a_2(w) \exp(-i w) \tag{3.15}$$

where $a_1(w)$ and $a_2(w)$ are functions of w which are to be determined in a convenient way. It follows that

$$\frac{d\varphi}{dw} = i a_1(w) \exp(i w) - i a_2(w) \exp(-i w) \tag{3.16}$$

if the following condition is imposed upon $a_1(w)$ and $a_2(w)$

$$\frac{da_1}{dw} \exp(i w) + \frac{da_2}{dw} \exp(-i w) = 0 \tag{3.17}$$

Thus the expression (3.16) is exactly the same as if the quantities $a_1(w)$ and $a_2(w)$ were constants. It is evident that

$$\left.\begin{aligned} \frac{da_1}{dw} &= \frac{1}{2} i \varepsilon \left\{ a_1 + a_2 \exp(-2i w) \right\} \\ \frac{da_2}{dw} &= -\frac{1}{2} i \varepsilon \left\{ a_2 + a_1 \exp(2i w) \right\} \end{aligned}\right\} \tag{3.18}$$

By introducing the column vector

$$\underset{\sim}{a}(w) = \begin{pmatrix} a_1(w) \\ a_2(w) \end{pmatrix} \tag{3.19}$$

and the matrix

$$\underset{\sim}{M}(w) = \frac{1}{2} i \begin{pmatrix} 1 & e^{-2i w} \\ -e^{2i w} & -1 \end{pmatrix} \tag{3.20}$$

with the properties

$$\left.\begin{aligned} \det \underset{\sim}{M}(w) &= 0 \\ \mathrm{Tr}\ \underset{\sim}{M}(w) &= 0 \end{aligned}\right\} \qquad (3.21)$$

Fröman writes the system of differential eqns.(3.18) in matrix form as

$$\frac{d\underset{\sim}{a}}{dw} = \underset{\sim}{M}(w)\,\underset{\sim}{a}(w) \qquad (3.22)$$

This differential equation can be replaced by the integral equation

$$\underset{\sim}{a}(w) = \underset{\sim}{a}(w_0) + \int_{w_0}^{w} dw_1\ \underset{\sim}{M}(w_1)\,\underset{\sim}{a}(w_1) \qquad (3.23)$$

the solution of which can be obtained by an iteration procedure and is

$$\underset{\sim}{a}(w) = \underset{\sim}{F}(w, w_0)\ \underset{\sim}{a}(w_0) \qquad (3.24)$$

Fröman points out that

$$\begin{aligned} &\frac{\partial}{\partial w}\,\underset{\sim}{F}(w, w_0) = \underset{\sim}{M}(w)\,\underset{\sim}{F}(w, w_0) \\ &\frac{\partial}{\partial w}\det \underset{\sim}{F}(w, w_0) = 0 \\ &\det \underset{\sim}{F}(w, w_0) = 1 \\ &\underset{\sim}{F}(w_0, w) = \left\{ F(w_0, w) \right\}^{-1} \end{aligned} \qquad (3.25)$$

Fröman then derives an expression for the general solution of the original differential eqn. (3.9). It is convenient here to introduce the row vector

$$f(z) = \begin{pmatrix} f_1(z) & f_2(z) \end{pmatrix} \tag{3.26}$$

where $f_1(z)$ and $f_2(z)$ are the J.W.K.B. functions defined by

$$\left.\begin{aligned} f_1(z) &= q(z)^{-\frac{1}{2}} \exp\{i w(z)\} \\ f_2(z) &= q(z)^{-\frac{1}{2}} \exp\{-i w(z)\} \end{aligned}\right\} \tag{3.27}$$

The general solution and its derivatives are

$$\left.\begin{aligned} \psi(z) &= a_1(z) f_1(z) + a_2(z) f_2(z) = f(z)\, \underset{\sim}{a}(z) \\ \psi'(z) &= a_1(z) f_1'(z) + a_2(z) f_2'(z) = f'(z)\, \underset{\sim}{a}(z) \end{aligned}\right\} \tag{3.28}$$

where

$$\underset{\sim}{a}(z) = \underset{\sim}{F}(z, z_0)\, \underset{\sim}{a}(z_0) \tag{3.29}$$

3.2.2 Basic Estimates of the "F-Matrix"

A convenient path Λ from z_0 to z (from w_0 to w) is chosen. This yields

$$\left.\begin{aligned} |F_{11}(w, w_0) - 1| &\le \frac{1}{2M}\left[\exp(M\mu) - 1\right] \\ |F_{12}(w, w_0)| &\le \frac{1}{2M}\left[\exp(M\mu) - 1\right] |\exp(-2iw_1)| \\ |F_{21}(w, w_0)| &\le \frac{1}{2M}\left[\exp(M\mu) - 1\right] |\exp(2iw)| \\ |F_{22}(w, w_0) - 1| &\le \frac{\mu}{2} + \frac{1}{2M}\left[\exp(M\mu) - 1 - M\mu\right] |\exp\{-2i(w - w_0)\}| \end{aligned}\right\} \tag{3.30}$$

where M is a number that

$$\frac{1}{2} \left| 1 - \exp\{-2i(w_{\nu+1} - w_\nu)\} \right| \le M \tag{3.31}$$

for any possible division of the path of integration and

$$\mu = \int_{w_0}^{w} |\varepsilon(w_1)|\, dw_1| \qquad (3.32)$$

M is chosen to be 1 if $\exp(iw)$ increases monotonically from z_0 to z along the path Λ. If $\mathrm{Im}(iw)$ is constant along Λ, which occurs for instance, in a classically forbidden region, we can choose $M = \frac{1}{2}$.

3.2.3 Estimates of the "F-Matrix" Connecting Two Points on Opposite Sides of a Classical Turning Point

Fröman estimates the elements of the matrix $\underset{\sim}{F}(x_1, x_2)$ where the points x_1 and x_2 lie on the real axis but on opposite sides of a classical turning point, which is assumed to correspond to a simple zero of $q^2(x)$, x_1 and x_2 lie far enough from the classical turning point for the J.W.K.B. approximation to be valid in the neighbourhood of x_1, as well as x_2. The situations depicted by Figs. 3.1 and 3.2 are considered. The basis estimates (3.25) yield

$$\left.\begin{aligned} |F_{11}(x_1, x_2) - 1| &\leq \mu + \text{higher powers of } \mu \\ |F_{12}(x_1, x_2)| &\leq |\exp\{2i\, w(x_1)\}| \left[\frac{\mu}{2} + \text{higher powers of } \mu\right] \end{aligned}\right\} \qquad (3.33)$$

if μ is small compared to 1. Furthermore,

$$\left.\begin{aligned} F_{12}(x_1, x_2) &= \pm i\, F_{11}^{*}(x_1, x_2) \\ F_{21}(x_1, x_2) &= \mp i\, F_{22}^{*}(x_1, x_2) \end{aligned}\right\} \qquad (3.34)$$

where the plus sign applies to Fig. 3.1 and the minus sign

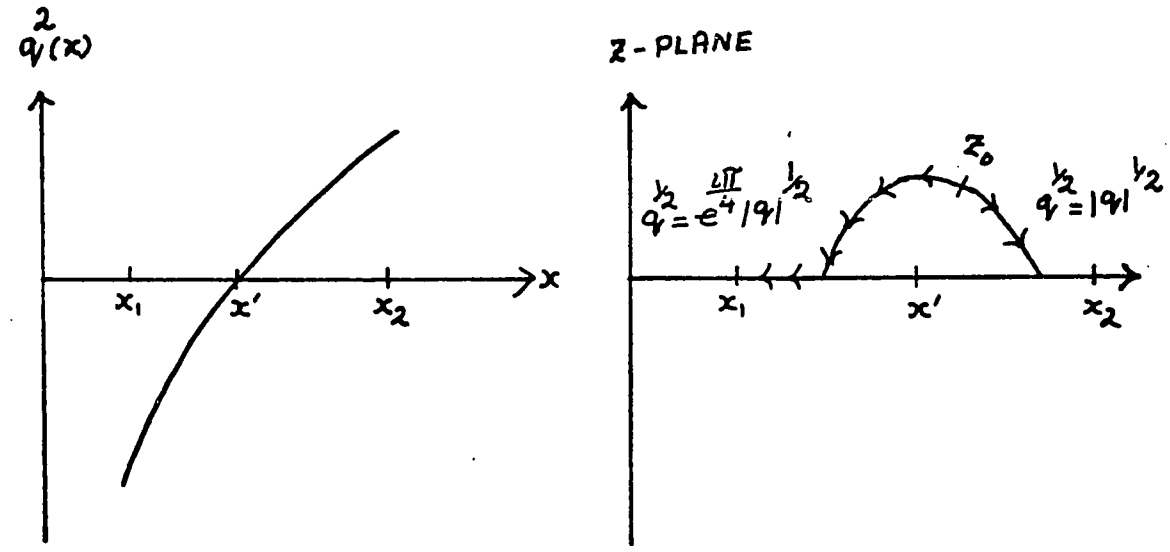

FIG. 3.1 Barrier to the Right

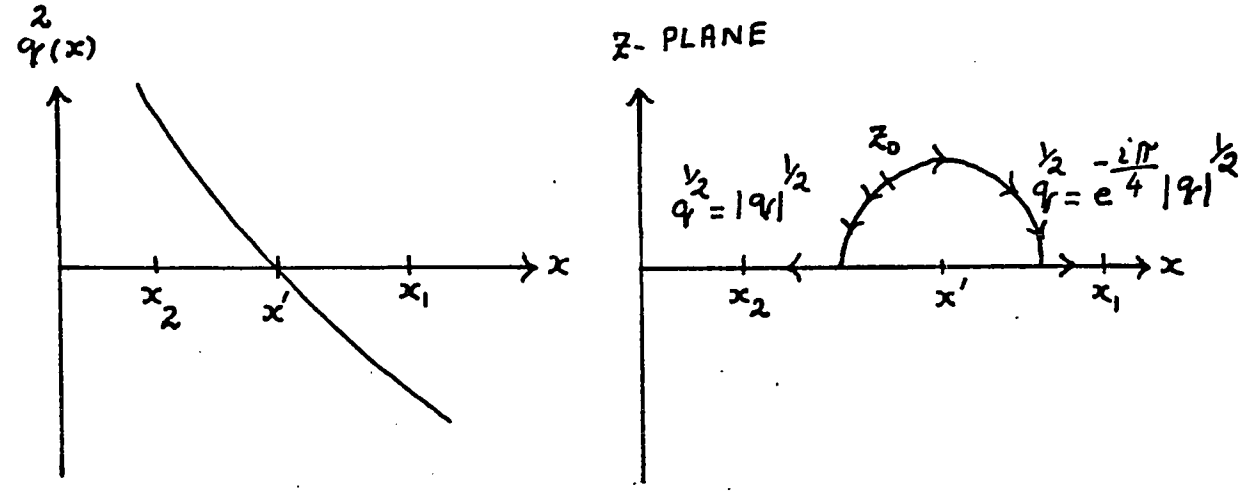

FIG. 3.2 Barrier to the Left

to Fig. 3.2. In other words

$$F_{11}(x_1, x_2) \simeq 1 \; ; \quad F_{12}(x_1, x_2) \simeq \pm i \tag{3.35}$$

whereas the elements $F_{22}(x_1, x_2)$ and $F_{21}(x_1, x_2)$ are undetermined.

3.2.4 Estimates of the "F-Matrix" Connecting Two Points on Opposite Sides of an Overdense Potential Barrier.

3.2.4.1 Well Separated Classical Turning Points

The situation is represented by Fig. 3.3.

$\underset{\sim}{F}(x_1, x_2)$ is written as

$$\underset{\sim}{F}(x_1, x_2) = \begin{pmatrix} -[1 + O(\mu)]\, e^{2K} & i + O(\mu) \\ [i + O(\mu)]\, e^{2K} & 1 + O(\mu) \end{pmatrix} \tag{3.36}$$

where K is $\int_{x'}^{x''} q(\xi)\, d\xi$. Here $\mu = \mu(x_1, x_2)$ is the μ-integral for the whole path Λ from x_1 to x_2. $O(\mu)$ denotes a quantity which is at the most of the order of magnitude of μ, even if μ cannot tend to the limit zero.

3.2.4.2 Classical Turning Points Close Together

The situation is illustrated by Fig. 3.4. The approximate formula below is obtained for the "F-Matrix"

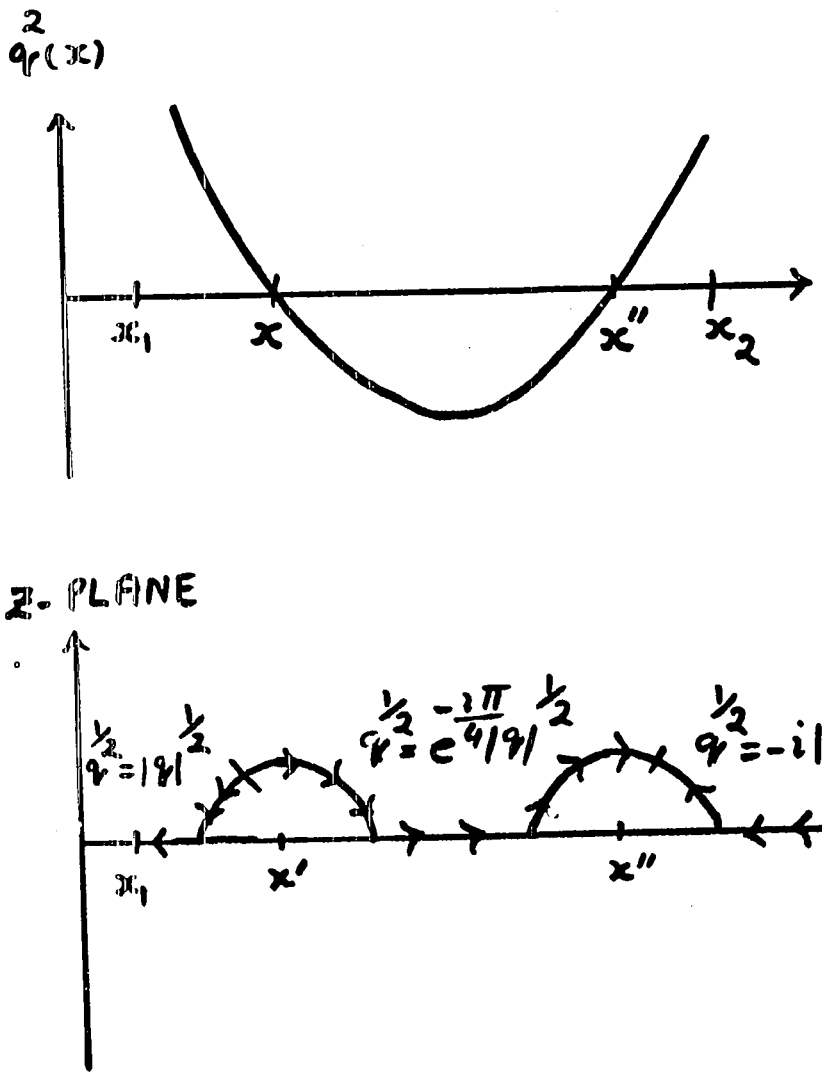

FIG. 3.3 Overdense Potential Barrier. x' and x'' Well Separated

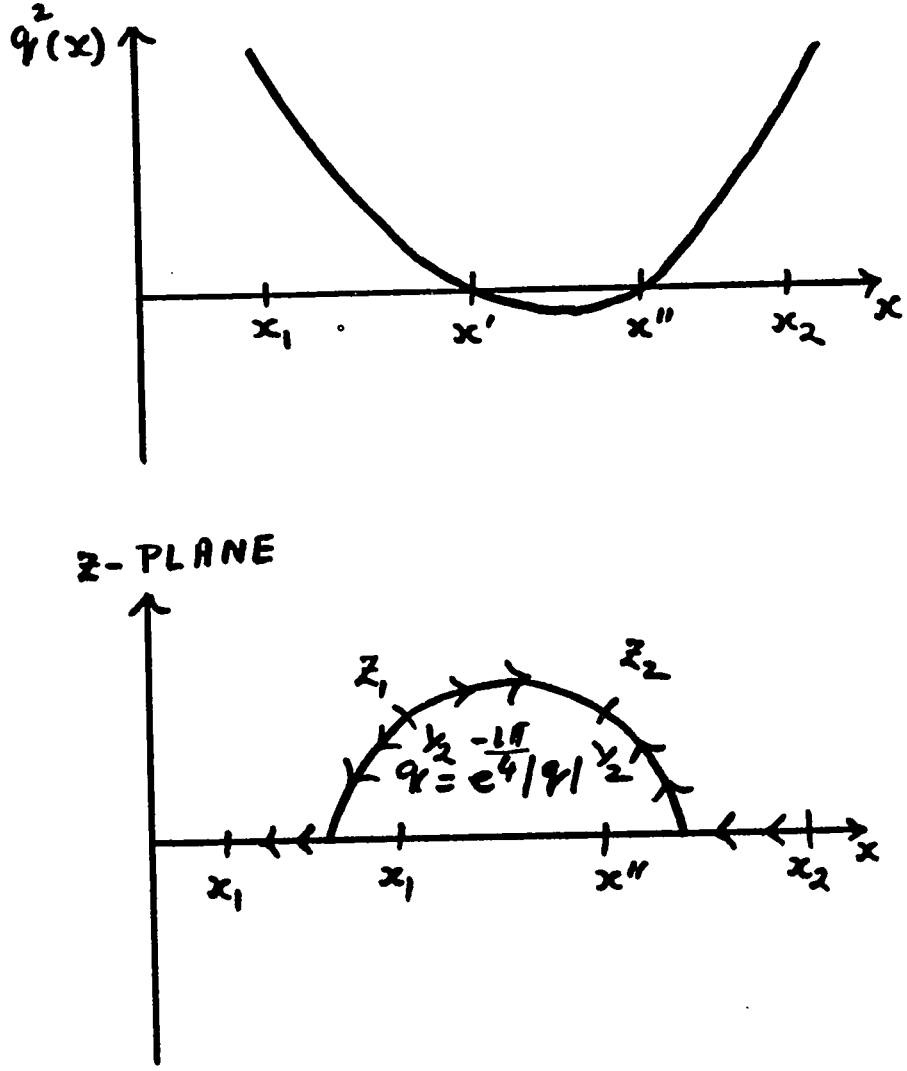

FIG. 3.4 Overdense Potential Barrier. x' and x'' Close Together

$$\underset{\sim}{F}(x_1,x_2) = \begin{pmatrix} -e^{2K} & e^{i\varphi}\{1+e^{-2K}\}^{\frac{1}{2}} \\ e^{-i\varphi}\{1+e^{-2K}\}^{\frac{1}{2}} & e^{2K} \quad 1 \end{pmatrix} \tag{3.37}$$

where $K = \int_{x'}^{x''} |q(\xi)|\, d\xi$.

3.2.5 Fröman's Connection Formulae [39,40,41]

Using these estimates and equations, Fröman derives the connection formulae as expressed below

$$\left.\begin{aligned} A|q(x)|^{-\frac{1}{2}} \exp\left\{ i\left(|w(x)|+\tfrac{\pi}{4}\right)\right\} + B|q(x)|^{-\frac{1}{2}} \exp\left\{-i\left(|w(x)|+\tfrac{\pi}{4}\right)\right\} &\rightarrow \\ \rightarrow (A+B)\ |q(x)|^{-\frac{1}{2}}\ \exp\{|w(x)|\} & \end{aligned}\right\} \tag{3.38}$$

$$|q(x)|^{-\frac{1}{2}} \cos\left[|w(x)|+\gamma-\tfrac{\pi}{4}\right] \rightarrow \sin\gamma\, |q(x)|^{-\frac{1}{2}} \exp|w(x)| \tag{3.39}$$

where γ is a real constant which must not be close to a multiple of π .

$$|q(x)|^{-\frac{1}{2}} \exp\{-|w(x)|\} \rightarrow 2|q(x)|^{-\frac{1}{2}} \cos\left[|w(x)|-\tfrac{\pi}{4}\right] \tag{3.40}$$

The above results are independent of the choice of the phase of $q(x)^{-\frac{1}{2}}$. It is primordial to note that these formulae can only be used if the classical turning points are well separated in a barrier penetration problem. The striking feature of these formulae is that they only are valid in the direction indicated by the arrow.

CHAPTER IV

J.W.K.B. PENETRABILITY CALCULATIONS

CHAPTER IV

J.W.K.B. PENETRABILITY CALCULATIONS

The penetrability of Strutinsky's fission barrier is a crucial quantity for the fission process, since it provides a possibility of estimating fission half-lives and isomeric lifetimes. It may be noted that the potential barrier of Fig. 2.3 is an asymmetric potential barrier.

4.1 J.W.K.B. CALCULATIONS WHEN THE CLASSICAL TURNING POINTS ARE WELL SEPARATED

The type of fission barrier considered is given in the Fig. 4.1. β is the prolate deformation coordinate in the fission direction. The points a, b, c and d in Fig. 4.1 are the classical turning points which separate the regions I,II,III,IV and V respectively. To avoid complication, the classical turning points are well separated and the incident energy E lies in the range of applicability of the J.W.K.B. approximation, i.e., between the bottom of the second potential well and the top of barrier B . We connect from right to left and at points

	$\beta = d$	the barrier is to the left
	$\beta = c$	to the right
	$\beta = b$	to the left
and	$\beta = a$	is to the right

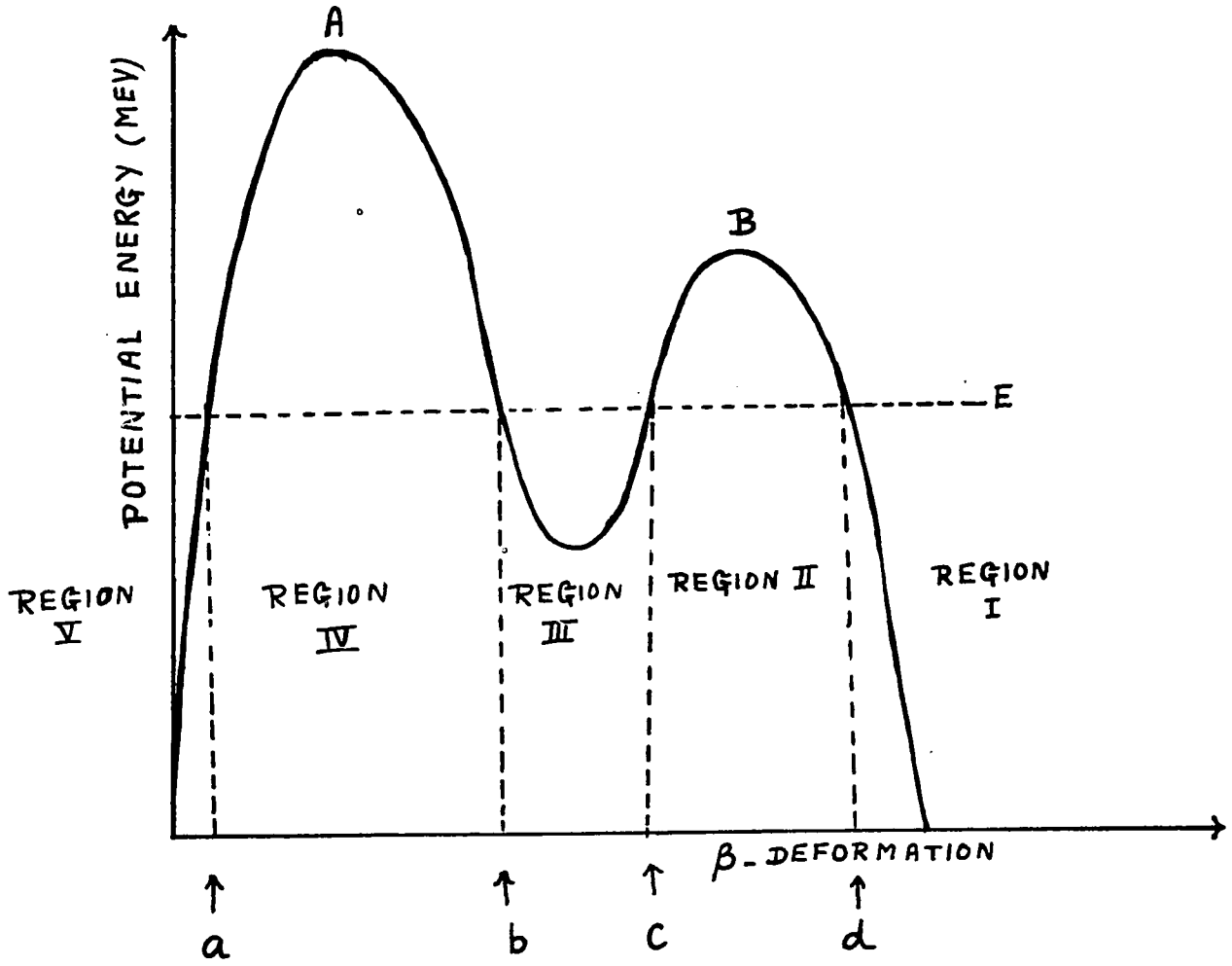

FIG. 4.1 The Double Hump Fission Barrier and The J.W.K.B. Approximation When the Classical Turning Points are Well Separated

4.1.1 Penetrability Calculations With Bohm's Connection Formulae [38]

To the right of the classical turning point d, i.e. in Region I, only a transmitted wave is present and in the J.W.K.B. approximation it is written as

$$\Psi_I \simeq \frac{A}{\sqrt{k}} \exp\left\{i\left(\int_d^\beta k\, d\beta - \pi/4\right)\right\} \tag{4.1}$$

where A is the amplitude of the transmitted wave; the phase factor $\pi/4$ is introduced for convenience in making connections. Ψ_I can also be written as

$$\Psi_I \simeq \frac{A}{\sqrt{k}}\left[\cos\left(\int_d^\beta k\, d\beta - \pi/4\right) + i\sin\left(\int_d^\beta k\, d\beta - \pi/4\right)\right] \tag{4.2}$$

At $\beta = d$, the barrier is to the left and the connection formulae (3.7) and (3.8) will yield Ψ_{II}.

$$\Psi_{II} \simeq \frac{A}{\sqrt{\chi}}\left[\frac{e^{-K_1}}{2}\exp\left(\int_c^\beta \chi\, d\beta\right) - i e^{K_1}\exp\left(-\int_c^\beta \chi\, d\beta\right)\right] \tag{4.3}$$

where

$$K_1 = \int_c^d \chi\, d\beta \tag{4.4}$$

At the point $\beta = c$, the barrier is to the right and the formulae (3.3), (3.4) and (3.5) are used. Ψ_{III} is then

$$\Psi_{III} \simeq \frac{A}{\sqrt{k}}\left[\cos\left(\int_b^\beta k\, d\beta - \pi/4\right)\left\{-\frac{e^{-K_1}}{2}\cos\phi - 2i e^{K_1}\sin\phi\right\} + \sin\left(\int_b^\beta k\, d\beta - \pi/4\right)\left\{-\frac{e^{-K_1}}{2}\sin\phi - 2i e^{K_1}\cos\phi\right\}\right] \tag{4.5}$$

where

$$\phi = \int_b^c k\, d\beta \tag{4.6}$$

The barrier is to the left of point $\beta = b$ and with the help of formulae(3.7) and (3.8) we obtain

$$\Psi_{IV} \simeq \frac{A}{\sqrt{\chi}} \left[e^{-K_2} \left\{ \frac{e^{-K_1}}{4} \cos\phi - i e^{K_1} \sin\phi \right\} \exp\left(\int_a^\beta \chi \, d\beta \right) + \right.$$
$$\left. + e^{K_2} \left\{ -\frac{e^{-K_1}}{2} \sin\phi - 2i e^{K_1} \cos\phi \right\} \exp\left(-\int_a^\beta \chi \, d\beta \right) \right] \qquad (4.7)$$

where

$$K_2 = \int_a^b \chi \, d\beta \qquad (4.8)$$

Finally using the formulae(3.3), (3.4) and (3.5) again since the barrier is to the left at point $\beta = a$, Ψ_V is obtained.

$$\Psi_V \simeq -\frac{A}{\sqrt{k}} \left[\left(\frac{e^{-[K_1+K_2]}}{4} \cos\phi - i e^{K_1-K_2} \sin\phi \right) \sin\left(\int_\beta^a k \, d\beta - \pi/4 \right) + \right.$$
$$\left. + \left(e^{K_2-K_1} \sin\phi + 4i e^{K_1+K_2} \cos\phi \right) \cos\left(\int_\beta^a k \, d\beta - \pi/4 \right) \right] \qquad (4.9)$$

Expanding $\sin\left(\int_\beta^a k \, d\beta - \pi/4 \right)$ and $\cos\left(\int_\beta^a k \, d\beta - \pi/4 \right)$ in terms of complex exponentials, Ψ_V can be transformed to

$$\Psi_V \simeq -\frac{A}{2\sqrt{k}} \exp\left\{ i \left(\int_\beta^a k \, d\beta - \pi/4 \right) \right\} \cdot$$
$$\cdot \left[i\cos\phi \left(4 e^{K_2+K_1} - \frac{1}{4} e^{-[K_1+K_2]} \right) + \sin\phi \left(e^{K_2-K_1} - e^{K_1-K_2} \right) \right] -$$
$$(4.10)$$
$$- \frac{A}{2\sqrt{k}} \exp\left\{ -i \left(\int_\beta^a k \, d\beta - \pi/4 \right) \right\} \cdot$$
$$\cdot \left[i\cos\phi \left(4 e^{K_2+K_1} + \frac{1}{4} e^{-[K_1+K_2]} \right) + \sin\phi \left(e^{K_2-K_1} + e^{K_1-K_2} \right) \right]$$

The penetrability of the barrier at the incident energy E is given by

$$P(E) = \frac{\left|\Psi_{TRANS}\sqrt{k_{TRANS}}\right|^2}{\left|\Psi_{INC}\sqrt{k_{INC}}\right|^2} = \frac{\left|\Psi_I\sqrt{k_{TRANS}}\right|^2}{\left|\text{incident part of } \Psi_I\sqrt{k_{INC}}\right|^2} \tag{4.11}$$

We observe that $\sqrt{k_{INC}} = \sqrt{k_{TRANS}}$; therefore

$$P(E) = \frac{\left|\Psi_I\right|^2}{\left|\text{incident part of } \Psi_I\right|^2} \tag{4.12}$$

The expression

$$\left.\begin{aligned} &-\frac{A}{2\sqrt{k}}\ \exp\left\{-i\left(\int_\beta^\alpha k\,d\beta - \pi/4\right)\right\}\cdot \\ &\cdot\left[i\cos\phi\left(4e^{K_1+K_2} + \tfrac{1}{4}e^{-[K_1+K_2]}\right) + \sin\phi\left(e^{K_2-K_1} + e^{K_1+K_2}\right)\right] \end{aligned}\right\} \tag{4.13}$$

represents the incident part of Ψ_I.

Further considerations yield

$$\left.\begin{aligned} P(E) = \frac{4}{\sin^2\phi\left(e^{2[K_1-K_2]} + e^{2[K_2-K_1]} + 2\right) +} \\ +\cos^2\phi\left(\frac{e^{-2[K_1+K_2]}}{16} + 16\,e^{2[K_1+K_2]} + 2\right) \end{aligned}\right\} \tag{4.14}$$

Ignatiuk [42] suggests that $P(E)$, the total penetrability of the fission barrier, can be expressed in terms of the penetrabilities P_A and P_B of barriers A and B, respectively.

A general expression for P_A and P_B goes as follows

$$P_A = \left(e^{K_1} + \frac{1}{4}\, e^{-K_1}\right)^{-2}$$

$$P_B = \left(e^{K_2} + \frac{1}{4}\, e^{-K_2}\right)^{-2} \qquad (4.15)$$

But if the J.W.K.B. approximation is to be valid [43], then

$$\int_c^d \chi\, d\beta \gg 1 \quad , \quad \int_a^b \chi\, d\beta \gg 1 \qquad (4.16)$$

Hence

$$P_A = e^{-2K_1} \quad , \quad P_B = e^{-2K_2} \qquad (4.17$$

and

$$P(E) = \frac{64\, P_A P_B}{\left[16\,(P_A + P_B)^2\right] \sin^2\phi + \cos^2\phi \left[(P_A P_B + 16)^2\right]} \qquad (4.18)$$

Ignatiuk's [42] results can be obtained by approximating eqn. (4.18) further. We know that $0 \leq P_A P_B \leq 1$ and $P_A P_B$ can be neglected compared to 16 in the multiplicator of the term $\cos^2\phi$. This gives

$$P(E) = \frac{1}{4}\, P_A P_B \left[\frac{(P_A + P_B)^2}{16} \sin^2\phi + \cos^2\phi\right] \qquad (4.19)$$

Although the results of these calculations are quoted in several papers [24,44,45] no derivation for the

penetrability in the J.W.K.B. approximation is published. It is of great interest to obtain the derivation of the penetrability of Strutinsky's potential barrier.

4.1.2 A Penetrability Calculation Using the Connection Formulae in the Correct Direction

To the right of point d, only a transmitted wave is present, we write

$$\Psi_I \simeq A\,|q(\beta)|^{-\frac{1}{2}} \exp\left\{ i\left(\int_d^\beta |q(\xi)|\,d\xi + \frac{\pi}{4}\right)\right\} \tag{4.20}$$

At $\beta = d$, the barrier is to the left. The connection formula used is

$$|q(\beta)|^{-\frac{1}{2}} \cos\left(\int_d^\beta |q(\xi)|\,d\xi + \gamma - \pi/4\right) \rightarrow |q(\beta)|^{-\frac{1}{2}} \sin\gamma \exp\left(\int_\beta^d |q(\xi)|\,d\xi\right) \tag{4.21}$$

If Ψ_I is transformed to

$$\Psi_I \simeq A\,|q(\beta)|^{-\frac{1}{2}} \left[\cos\left(\int_d^\beta |q(\xi)|\,d\xi + \pi/4\right) + i\sin\left(\int_d^\beta |q(\xi)|\,d\xi + \frac{\pi}{4}\right)\right] \tag{4.22}$$

and if γ is put equal to $\frac{\pi}{2}$ in eqn.(4.21), after connection

$$\Psi_{II} \simeq A\,|q(\beta)|^{-\frac{1}{2}} \sin\pi/2 \exp\left(\int_\beta^d |q(\xi)|\,d\xi\right) \tag{4.23}$$

or

$$\Psi_{II} \simeq A\,|q(\beta)|^{-\frac{1}{2}} \exp\left(\int_\beta^c |q(\xi)|\,d\xi\right) \exp\left(\int_c^d |q(\xi)|\,d\xi\right. \tag{4.24}$$

At $\beta = c$, the barrier is to the right and the connection formula

$$|q(\beta)|^{-\frac{1}{2}} \exp\left(-\int_c^{\beta} |q(\xi)| d\xi\right) \rightarrow 2|q(\beta)|^{-\frac{1}{2}} \left(\cos \int_{\beta}^{c} |q(\xi)| d\xi - \pi/4\right) \quad (4.25)$$

gives

$$\psi_{III} \simeq A |q(\beta)|^{-\frac{1}{2}} \; 2 \exp\left(\int_c^{d} |q(\xi)| d\xi\right) \cos\left(\int_{\beta}^{c} |q(\xi)| d\xi - \pi/4\right) \quad (4.26)$$

or

$$\left.\begin{aligned} \psi_{III} \simeq 2A |q(\beta)|^{-\frac{1}{2}} \exp\left(\int_c^{d} |q(\xi)| d\xi\right) \cdot \Big[& \sin\phi \cos\left(\int_b^{\beta} |q(\xi)| d\xi - \pi/4\right) \\ & - \cos\phi \sin\left(\int_b^{\beta} |q(\xi)| d\xi - \pi/4\right) \Big] \end{aligned}\right\} \quad (4.27)$$

where ϕ is defined by $\int_b^c |q(\xi)| d\xi$

At $\beta = b$, the connection formula

$$\left.\begin{aligned} & |q(\beta)|^{-\frac{1}{2}} \cos\left(\int_b^{\beta} |q(\xi)| d\xi - \frac{\pi}{4} + \gamma\right) \longrightarrow \\ & \longrightarrow |q(\beta)|^{-\frac{1}{2}} \sin\gamma \exp\left(\int_{\beta}^{b} |q(\xi)| d\xi\right) \end{aligned}\right\} \quad (4.28)$$

with $\gamma = \frac{\pi}{2}$, applies since at $\beta = b$, the barrier is to the left. It can also be expressed as

$$-|q(\beta)|^{-\frac{1}{2}} \sin\left(\int_b^{\beta} |q(\xi)| d\xi - \pi/4\right) \rightarrow |q(\beta)|^{-\frac{1}{2}} \exp\left(\int_{\beta}^{b} |q(\xi)| d\xi\right) \quad (4.29)$$

Hence,

$$\Psi_{IV} \simeq 2A\,|q(\beta)|^{-\frac{1}{2}}\ \exp\left(\int_c^d |q(\xi)|\,d\xi\right)\cdot$$

$$\cdot\ \exp\left(\int_a^b |q(\xi)|\,d\xi\right)\ \cos\phi\ \exp\left(\int_\beta^a |q(\xi)|\,d\xi\right) \qquad (4.30)$$

The connection formula used at the point $\beta = a$, where the barrier is to the right, is

$$|q(\beta)|^{-\frac{1}{2}}\ \exp\left(-\int_a^\beta |q(\xi)|\,d\xi\right) \rightarrow$$

$$\rightarrow 2\,|q(\beta)|^{-\frac{1}{2}}\ \cos\left(\int_\beta^a |q(\xi)|\,d\xi - \pi/4\right) \qquad (4.31)$$

$$\rightarrow 2\,|q(\beta)|^{-\frac{1}{2}}\ \cos\left(\int_a^\beta q(\xi)\,d\xi + \frac{\pi}{4}\right)$$

Now

$$\Psi_{V} \simeq 4A\,|q(\beta)|^{-\frac{1}{2}}\ \exp\left(\int_c^d |q(\xi)|\,d\xi\right)\cdot$$

$$\cdot\ \exp\left(\int_a^b |q(\xi)|\,d\xi\right)\ \cos\phi\ \cos\left(\int_a^\beta |q(\xi)|\,d\xi + \pi/4\right) \qquad (4.32)$$

The penetrability is expressed as follows

$$P(E) = \frac{|\sqrt{k_{TRANS}}|^2\ |\Psi_{TRANS}|^2}{|\sqrt{k_{INC}}|^2\ |\Psi_{INC}|^2} = \frac{|\Psi_I|^2}{|\text{incident part of } \Psi_I|^2} \qquad (4.33)$$

since $k_{TRANS} = k_{INC}$ in the J.W.K.B. approximation. The incident part of Ψ_V is obtained by expanding $\cos\left(\int_a^\beta |q(\xi)|\,d\xi + \frac{\pi}{4}\right)$ in terms of complex exponentials and reads

$$2A\,|q(\beta)|^{-\frac{1}{2}}\,\exp\left(\int_c^d |q(\bar{r})|\,d\bar{r}\right)\,\exp\left(\int_a^b |q(\bar{r})|\,d\bar{r}\right)\cdot$$

$$\cdot\left[\exp\left\{i\left(\int_a^\beta q(\bar{r})\,d\bar{r}+\tfrac{\pi}{4}\right)\right\}+\exp\left\{-i\left(\int_a^\beta q(\bar{r})\,d\bar{r}+\tfrac{\pi}{4}\right)\right\}\right] \qquad (4.34)$$

P_A and P_B are exactly equal to

$$P_A=\exp\left(-2\int_a^b |q(\bar{r})|\,d\bar{r}\right)$$

$$P_B=\exp\left(-2\int_c^d q(\bar{r})\,d\bar{r}\right) \qquad (4.35)$$

Thus,

$$P(E)=\frac{\exp\left(-2\int_a^b |q(\bar{r})|\,d\bar{r}\right)\cdot\exp\left(-2\int_c^d |q(\bar{r})|\,d\bar{r}\right)}{4\cos^2\phi} \qquad (4.36)$$

$$P(E)=\frac{P_A\,P_B}{4\cos^2\phi}$$

4.2 J.W.K.B. CALCULATION OF THE PENETRABILITY WHEN THE CLASSICAL TURNING POINTS c AND d ARE CLOSE TOGETHER

The fission barrier considered is depicted in Fig. 4.2. Let us pay special attention to barrier β and the wave function on both sides of the second maximum. The classical turning points c and d are close together. Fröman's "F-Matrix" formalism[39] is applied here. The situation at barrier β is illustrated in Fig. 4.3.

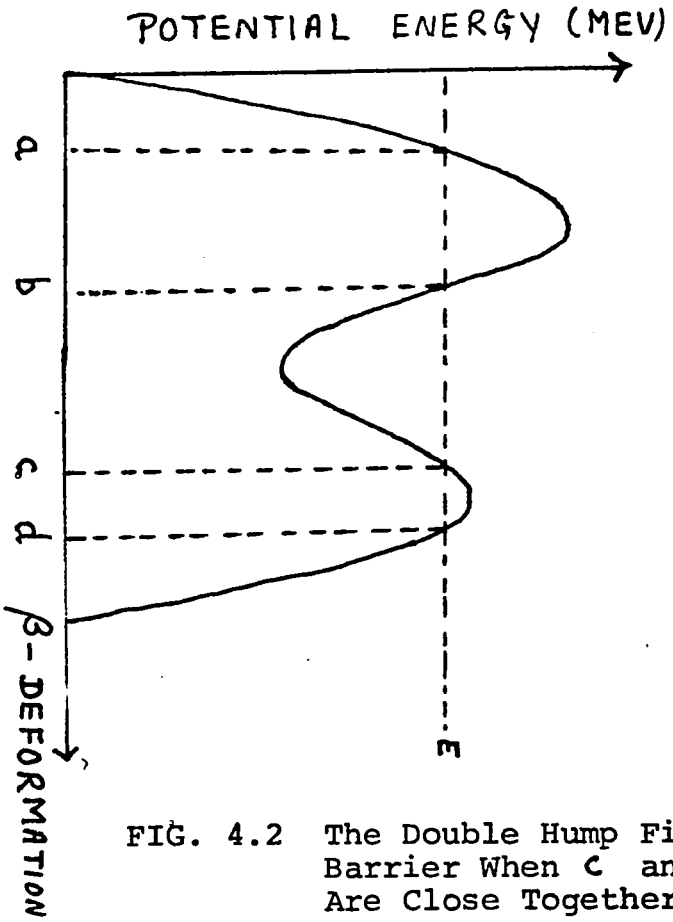

FIG. 4.2 The Double Hump Fission Barrier When c and d Are Close Together

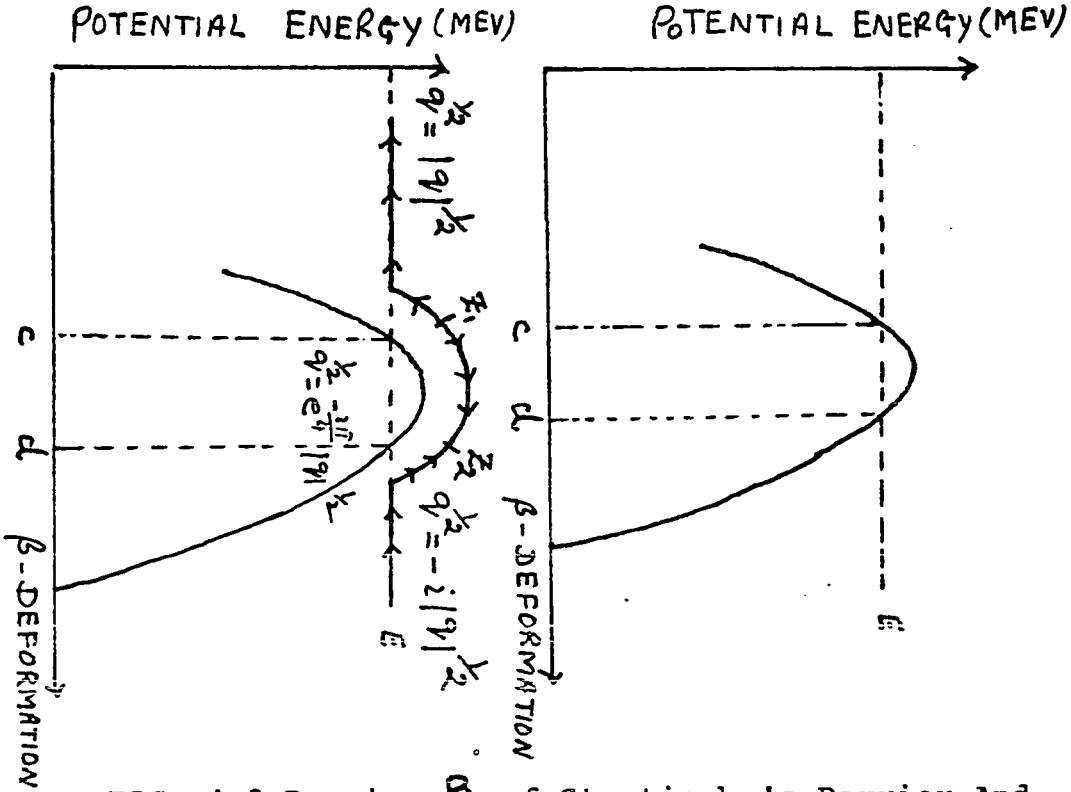

FIG. 4.3 Barrier B of Strutinsky's Barrier And Quantities for the "F-Matrix" Formalism

We have the following expression for $\psi(\beta)$ on the real β axis

$$\left.\begin{aligned}\psi(\beta) &= a_1(\beta)\, f_1(\beta) + a_2(\beta)\, f_2(\beta) \\ &= \underset{\sim}{f}(\beta)\ \ \underset{\sim}{a}(\beta) \\ &= \underset{\sim}{f}(\beta)\ \ \underset{\sim}{F}(\beta, +\infty)\ \underset{\sim}{a}(+\infty) \\ &= \underset{\sim}{f}(\beta)\ \ \underset{\sim}{F}(\beta, +\infty) \begin{pmatrix} a_1(+\infty) \\ a_2(+\infty) \end{pmatrix}\end{aligned}\right\} \quad (4.37)$$

Far to the left of the barrier $(\beta > d)$, $f_1(\beta)$ represents a wave travelling from left to right and $f_2(\beta)$ represents a wave travelling from right to left. Far to the right of the barrier $(\beta < c)$ the opposite is true. Far to the right of the barrier, there shall be only an outgoing wave and therefore

$$a_1(+\infty) = 0$$

Hence

$$\left.\begin{aligned} a_1(\beta) &= F_{12}(\beta, +\infty)\ a_2(+\infty) \\ a_2(\beta) &= F_{22}(\beta, +\infty)\ a_2(+\infty)\end{aligned}\right\} \quad (4.38)$$

We choose the lower limit in $\omega(\beta)$ to be the left classical turning point C. For $\beta < c$, the function $\omega(\beta) = \int_c^\beta q(z)\, dz$ is real and for $\beta > d$, the same wave function has a constant imaginary part $-i K_2$ where K_2 is given by

$$K_2 = \int_c^d |q(\xi)|\, d\xi \qquad (4.39)$$

We now can write $\psi(\beta)$ as

$$\left.\begin{aligned}\psi(\beta) = a_2(+\infty)\,|q(\beta)|^{-\frac{1}{2}}\Big[&F_{12}(\beta,+\infty)\exp\left(i\int_c^{\beta} q(\zeta)\,d\zeta\right)\\ &+F_{22}(\beta,+\infty)\exp-\left(i\int_c^{\beta} q(\zeta)\,d\zeta\right)\Big]\end{aligned}\right\}(4.40)$$

If β lies to the right of the barrier, we have according to eqn. (3.23)

$$\left.\begin{aligned}F_{22}(\beta,+\infty) &= 1+O(\mu)\\ F_{12}(\beta,+\infty) &= e^{-2K_2}O(\mu)\end{aligned}\right\}(4.41)$$

Therefore

$$\psi(\beta) = i\,a_2(+\infty)\,|q(\beta)|^{-\frac{1}{2}}\,e^{-K_2}\exp\left(i\int_d^{\beta}|q(\xi)|\,d\xi\right)\left[1+O(\mu)\right] \quad (4.42)$$

or neglecting terms of order μ

$$\psi(\beta) = i\,a_2(+\infty)\,|q(\beta)|^{-\frac{1}{2}}\,e^{-K_2}\exp\left(i\int_d^{\beta}|q(\xi)|\,d\xi\right) \quad (4.43)$$

valid for $\beta > d$. Note the phase of $q(\beta)$ is taken directly from Fig. 4.3. On the other hand, if β lies to the left of the potential barrier and as the turning points are close together

$$\left.\begin{aligned} F_{22}(\beta, +\infty) &= 1 + o(\mu) \\ F_{12}(\beta, +\infty) &= e^{i\varphi}\left[1+e^{-2K_2}\right]^{\frac{1}{2}}\left[1+o(\mu)\right] \end{aligned}\right\} \quad (4.44)$$

The classical turning points c and d being close together, the phase φ is equal to $\frac{\pi}{2}$.[39] This reasoning yields the following expression for $\psi(\beta)$, valid if $\beta < c$.

$$\left.\begin{aligned} \psi(\beta) = |q(\beta)|^{-\frac{1}{2}} \; a_2(+\infty)\Big[e^{-i\frac{\pi}{4}} \exp\Big(-i\int_c^\beta |q(\xi)|\,d\xi\Big)\cdot \\ \cdot\left[1+o(\mu)\right] + \left(1+e^{-2K_2}\right)^{\frac{1}{2}} e^{i\varphi} \exp\Big(i\int_c^\beta |q(\xi)|\,d\xi\Big)\left[1+o(\mu)\right]\Big] \end{aligned}\right\} \quad (4.45)$$

or neglecting terms of order μ and replacing φ by $\frac{\pi}{2}$,

$$\left.\begin{aligned} \psi(\beta) = |q(\beta)|^{-\frac{1}{2}} \; a_2(+\infty)\Big[e^{-i\frac{\pi}{4}} \cdot \\ \cdot \exp\Big(-i\int_c^\beta |q(\xi)|\,d\xi\Big) + e^{i\frac{\pi}{2}}\left(1+e^{-2K_2}\right)^{\frac{1}{2}} \cdot \\ \cdot \exp\Big(i\int_c^\beta |q(\xi)|\,d\xi\Big)\Big] \end{aligned}\right\} \quad (4.46)$$

We normalize $\psi(\beta)$ conveniently by putting

$$a_2(+\infty) = e^{K - i\frac{\pi}{4}} \quad (4.47)$$

This yields

$$\psi(\beta) = |q(\beta)|^{-\frac{1}{2}} \exp\left\{i\left(\int_{\alpha}^{\beta} |q(\xi)|\, d\xi + \pi/4\right)\right\} \qquad (4.48)$$

valid for $\beta > \alpha$.

And

$$\psi(\beta) = |q(\beta)|^{-\frac{1}{2}} e^{K_2}\left[e^{-i\frac{\pi}{2}} \exp\left\{-i\left(\int_{c}^{\beta} |q(\xi)|\, d\xi + \pi/4\right)\right\}\cdot\right.$$
$$\left.\cdot\left(1+e^{-2K_2}\right)^{+\frac{1}{2}} \exp\left\{i\left(\int_{c}^{\beta} |q(\xi)|\, d\xi + \pi/4\right)\right\}\right] \qquad (4.49)$$

valid for $\beta < c$.

The connection formulae so far used fail in cases where the turning points are close together. We got around the difficulty by using Fröman's "F-Matrix" formalism.[39] The results of this procedure yield the following expressions fo: the wave functions in Regions I and III

$$\psi_{I} \simeq |q(\beta)|^{-\frac{1}{2}} \exp\left\{i\left(\int_{\alpha}^{\beta} |q(\xi)|\, d\xi + \pi/4\right)\right\} \qquad (4.48)(a)$$

$$\psi_{III} \simeq |q(\beta)|^{-\frac{1}{2}} e^{K_2}\left[-i \exp\left\{-i\left(\int_{c}^{\beta} |q(\xi)|\, d\xi + \pi/4\right)\right\} + \right.$$
$$\left. + \left(1+e^{2K_2}\right)^{+\frac{1}{2}} \exp\left\{i\left(\int_{c}^{\beta} |q(\xi)|\, d\xi + \pi/4\right)\right\}\right] \qquad (4.49)(a)$$

Let us write Ψ_{III} as below

$$\Psi_{III} \simeq |q(\beta)|^{-\frac{1}{2}} e^{K_2} \left[-i e^{i\phi} \exp\left\{-i\left(\int_b^\beta |q(\xi)|\,d\xi + \pi/4\right)\right\} + \right. \\ \left. + \left(1 + e^{-2K_2}\right)^{\frac{1}{2}} e^{-i\phi} \exp\left\{i\left(\int_b^\beta |q(\xi)|\,d\xi + \pi/4\right)\right\}\right] \tag{4.50}$$

where $$\phi = \int_b^c |q(\xi)|\,d\xi \tag{4.50a}$$

We will now use Fröman's one-directional connection formulae to connect the wave function in Region III, as given by eqn. (4.9) to the wave function in Region IV. The same connection formulae will also be used to connect Ψ_{IV} to Ψ_V. At $\beta = b$, the barrier is to the left and the connection formula

$$A|q(\beta)|^{-\frac{1}{2}} \exp\left\{i\left(\int_b^\beta |q(\xi)|\,d\xi + \pi/4\right)\right\} + B|q(\beta)|^{-\frac{1}{2}} \cdot \\ \cdot \exp\left\{-i\left(\int_b^\beta |q(\xi)|\,d\xi + \pi/4\right)\right\} \rightarrow (A+B)|q(\beta)|^{-\frac{1}{2}} \exp\left(\int_\beta^b |q(\xi)|\,d\xi\right) \tag{4.51}$$

is used. This yields the following expression for

$$\Psi_{IV} \simeq |q(\beta)|^{-\frac{1}{2}} \quad e^{K_2}\left(-i e^{i\phi} + \left[1 + e^{-2K_2}\right]^{\frac{1}{2}} e^{-i\phi}\right) \cdot \\ \cdot \exp\left(\int_\beta^b |q(\xi)|\,d\xi\right) \tag{4.52}$$

or

$$\Psi_{IV} \simeq |q(\beta)|^{-\frac{1}{2}} \quad e^{K_2}\left(-i e^{i\phi} + \left[1 + e^{-2K_2}\right]^{\frac{1}{2}} e^{-i\phi}\right) \cdot \\ \cdot e^{K_1} \exp -\left(\int_a^\beta |q(\xi)|\,d\xi\right) \tag{4.52a}$$

where

$$K_1 = \int_a^b |q(\xi)|\, d\xi \tag{4.53}$$

The barrier is to the right of the classical turning point $\beta = a$ and

$$\left.\begin{aligned} |q(\beta)|^{-\frac{1}{2}} \exp\left(-\int_a^\beta |q(\xi)|\, d\xi\right) &\longrightarrow \\ &\longrightarrow 2\,|q(\beta)|^{-\frac{1}{2}} \cos\left(\int_\beta^a |q(\xi)|\, d\xi - \tfrac{\pi}{4}\right) \\ &\longrightarrow 2\,|q(\beta)|^{-\frac{1}{2}} \cos\left(\int_a^\beta |q(\xi)|\, d\xi + \tfrac{\pi}{4}\right) \end{aligned}\right\} \tag{4.54}$$

Finally,

$$\left.\begin{aligned} \psi_I \simeq 2\,|q(\beta)|^{-\frac{1}{2}} \Big[e^{K_2} \Big(-i e^{i\phi} + \\ + \left[1 + e^{-2K_2}\right]^{+\frac{1}{2}} e^{-i\phi} \Big) e^{K_1} \Big] \cos\left(\int_a^\beta |q(\xi)|\, d\xi + \tfrac{\pi}{4}\right) \end{aligned}\right\} \tag{4.55}$$

The penetrability is given by

$$P(E) = \frac{|\sqrt{k_{TRANS}}|^2 \; |\psi_{TRANS}|^2}{|\sqrt{k_{INC}}|^2 \; |\psi_{INC}|^2} = \frac{|\psi_{TRANS}|^2}{|\psi_{INC}|^2} \tag{4.56}$$

since $\sqrt{k_{TRANS}} = \sqrt{k_{INC}}$ and where

$$\psi_{TRANS} \simeq |q(b)|^{-\frac{1}{2}} \exp\left\{i\left(\int_a^b |q(\xi)|\,d\xi + \tfrac{\pi}{4}\right)\right\} \qquad (4.43)\,(a)$$

$$\left.\begin{aligned} \psi_{INC} \simeq |q(b)|^{-\frac{1}{2}} \Big[& e^{K_2}\left(-i e^{i\phi} + \right. \\ & \left. + \left[1 + e^{-2K_2}\right]^{+\frac{1}{2}} e^{-i\phi}\right) e^{K_1}\Big]. \\ \cdot \exp\Big\{ & i\left(\int_a^b |q(\xi)|\,d\xi + \tfrac{\pi}{4}\right)\Big\} \end{aligned}\right\} (4.57)$$

Then,

$$P(E) = \frac{1}{\left| e^{K_1+K_2}\left(-i e^{i\phi} + \left[1 + e^{-2K_2}\right]^{+\frac{1}{2}} e^{-i\phi}\right)\right|^2}$$

$$\left.\begin{aligned} P(E) = \frac{e^{-2[K_1+K_2]}}{\Big| \Big[\sin\phi + \cos\phi \left(1+e^{-2K_2}\right)^{+\frac{1}{2}}\Big] - \right.} \\ \left. - i\left[\sin\phi\left(1+e^{-2K_2}\right)^{+\frac{1}{2}} + \cos\phi\right]\Big|^2 \end{aligned}\right\} (4.58)$$

After some algebra, we obtain

$$P(E) = \frac{e^{-2(K_1 + K_2)}}{1 + (1 + e^{-2K_2}) + 4(1+e^{-2K_2})^{\frac{1}{2}} \sin\phi \cos\phi} \tag{4.59}$$

Again we will express $P(E)$ in terms of P_A and P_B . P_A is as usual

$$P_A = e^{-2K_1} \tag{4.60}$$

but P_B is radically different from e^{-2K_2} since the classical turning points are close together.

P_B is expressed as

$$\left.\begin{aligned} P_B &= \frac{\left|\sqrt{k}_{TRANS\ at\ B}\right|^2 \left|\psi_{TRANS\ at\ B}\right|^2}{\left|\sqrt{k}_{INC\ at\ B}\right|^2 \left|\psi_{INC\ at\ B}\right|^2} \\ &= \frac{\left|\Psi_I\right|^2}{\left|\psi_{INC\ at\ B}\right|^2} \end{aligned}\right\} \tag{4.61}$$

"ψ_{INC} at B" is given by the expression

$$|q(B)|^{-\frac{1}{2}} e^{K_2} (1+e^{-2K_2})^{\frac{1}{2}} \exp\left\{i\left(\int_C^B |q(\bar{r})|\, d\bar{r} + \frac{\pi}{4}\right)\right\} \tag{4.62}$$

out of eqn. (4.50)

Hence,

$$P_D = \frac{1}{e^{2K_2}(1+e^{-2K_2})} \equiv \frac{1}{1+e^{2K_2}} \tag{4.63}$$

or

$$e^{-2K_2} = \frac{P_B}{1-P_B} \quad , \quad 1+e^{-2K_2} = \frac{1}{1-P_B} \tag{4.64}$$

These specifications yield

$$P(E) = \frac{P_A P_B}{(2-P_B) + 4\cos\phi \sin\phi \,(1-P_B)^{\frac{1}{2}}} \tag{4.65}$$

An interesting result is obtained if we go to the limit where c and d coincide, in this case $K_2 = 0$ and

$$P_B = \frac{1}{2} \tag{4.66}$$

Therefore,

$$P(E) = \frac{P_A}{3 + 2\cos\phi \sin\phi} \tag{4.67}$$

CHAPTER V

A GENERALIZATION OF CRAMER AND NIX METHOD OF CALCULATING PENETRABILITY THROUGH TWO-PEAKED FISSION BARRIERS

CHAPTER V

A GENERALIZATION OF CRAMER AND NIX METHOD OF CALCULATING PENETRABILITY THROUGH TWO-PEAKED FISSION BARRIERS

5.1 CRAMER AND NIX [45] METHOD

5.1.1 The Method

Cramer and Nix [45] claim to have found an exact method of calculating penetrabilities through the two-peaked fission barrier, shown in Fig. 5.1.

The barrier is parametrized by portions of three smoothly joined parabolas. The connecting points a and b define three regions of the potential energy. This potential energy is then written

$$V(\beta) = E_i \pm \frac{1}{2} \mu \omega_i^2 (\beta - \beta_i)^2 \qquad (5.1)$$

where β denotes the nuclear-deformation coordinate in the fission degree of freedom. The three regions $i = 1, 2, 3$ are separated by the connecting points a and b of the three parabolic curves shown in Fig. 5.1. The minus sign in eqn. (5.1) refers to the two peak regions (Regions I and III) and the plus sign refers to the region of the intermediate well (Region II). The energies E_i are the maximum or minimum values of the potential at the deformations β_i, the "frequencies" ω_i determine the widths of the individual

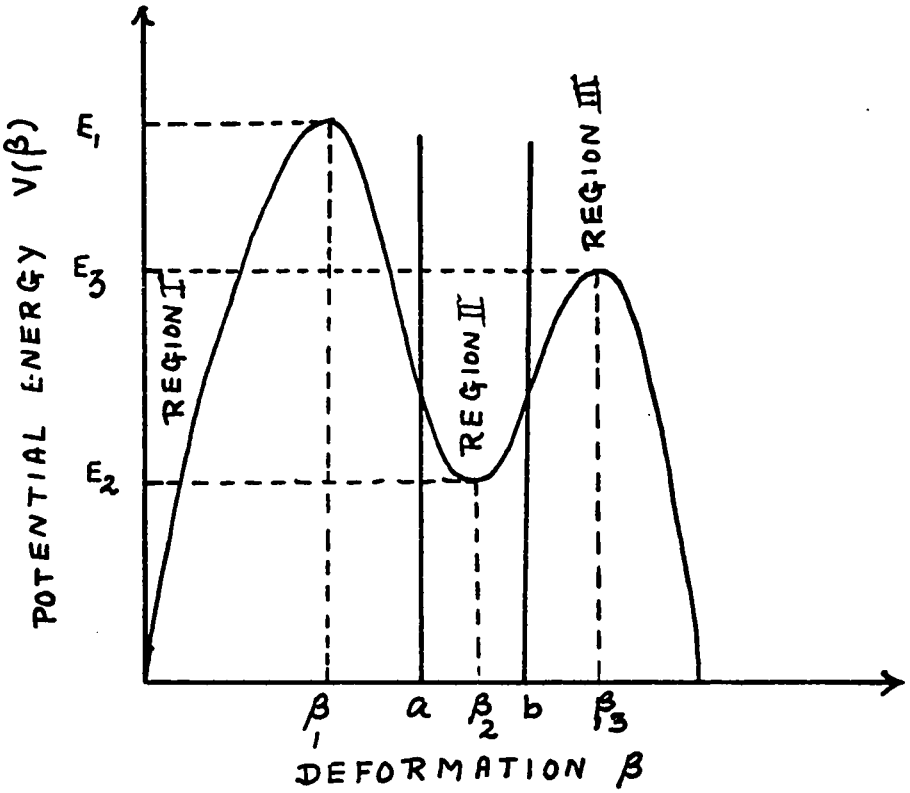

FIG. 5.1 Cramer and Nix Fission Barrier

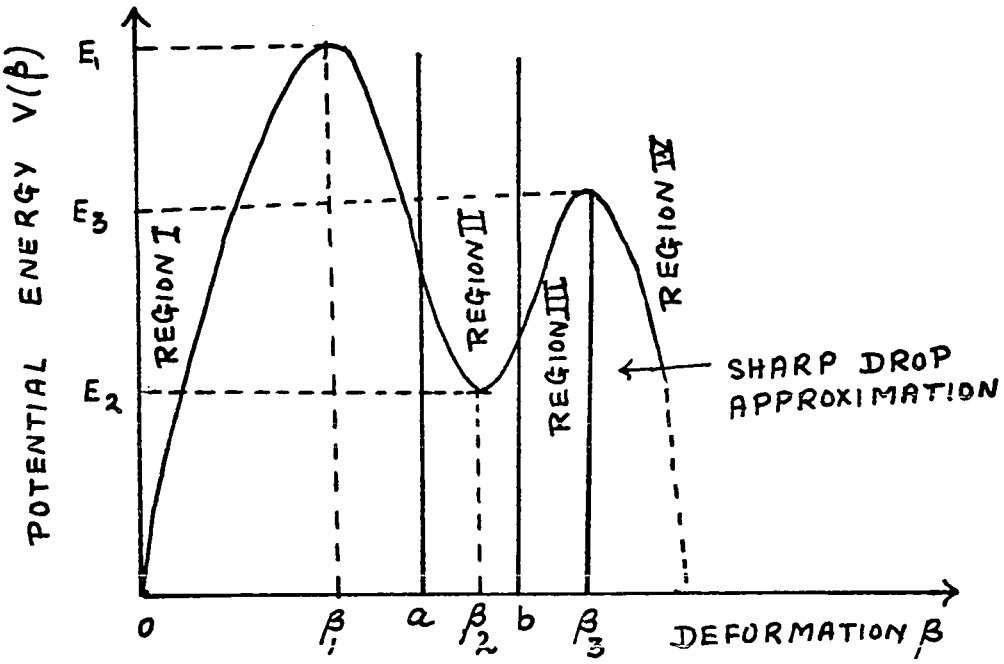

FIG. 5.2 The Sharp Drop Approximation

portions of the barrier. The inertial parameter μ represents the effective mass of the system with respect to distortions in the β direction. Hence $V(\beta)$ is explicitly written as

$$\left.\begin{aligned} V(\beta) &= E_1 - \tfrac{1}{2}\mu\omega_1^2(\beta-\beta_1)^2 && \beta \leq a \\ &= E_2 + \tfrac{1}{2}\mu\omega_2^2(\beta-\beta_2)^2 && a \leq \beta \leq b \\ &= E_3 - \tfrac{1}{2}\mu\omega_3^2(\beta-\beta_3)^2 && b \leq \beta \end{aligned}\right\} \quad (5.2)$$

The smooth joining of the parabolas is secured by requiring that $V(\beta)$ and its first derivatives with respect to β be continuous at points a and b. Cramer and Nix choose six basic parameters in function of which all other quantities are expressed. They are E_1, E_2 and E_3, and ω_1, ω_2 and ω_3. These parameters are fixed semiempirically. Since μ is assumed to be constant, an exact solution of the Schrödinger equation of the system is possible. The Schrödinger equation is

$$\frac{d^2}{d\beta_2}\psi_i + \frac{2\mu}{\hbar^2}\left[E - E_i \pm \tfrac{1}{2}\mu\omega_i^2(\beta-\beta_i)^2\right]\psi_i = 0 \quad (5.3)$$

where the plus sign applies when i refers to Region I and III and the minus sign when i refers to Region III. It is important to note that Cramer and Nix assume an incident wave of unit amplitude and take the reflection coefficient R to be zero in Region III. Eqn. (5.3) yields solutions of the form

$$\left.\begin{aligned} \Psi_I &= F\,\psi_1(\rightarrow) + B\,\varphi_1(\leftarrow) && \beta \leq a \\ \Psi_{II} &= C\,\delta_2 + D\,\eta_2 && a \leq \beta \leq b \\ \Psi_{III} &= T\,\psi_3(\rightarrow) && b \leq \beta \end{aligned}\right\} \quad (5.4)$$

The arrows indicate the direction of the phase velocity.

Equation (5.3) represents a general class of second order differential equations which in standard form are

$$\left.\begin{aligned} \frac{d^2y}{du^2} + \left(\tfrac{1}{4}u^2 - \alpha\right) y &= 0 && \beta \leq a \\ \frac{d^2y}{dv^2} - \left(\tfrac{1}{4}v^2 + \alpha\right) y &= 0 && a \leq \beta \leq b \\ \frac{d^2y}{dw^2} + \left(\tfrac{1}{4}w^2 - \alpha\right) y &= 0 && b \leq \beta \end{aligned}\right\} \quad (5.5)$$

The solutions of these equations are Weber parabolic cylinder functions.[46] * To reduce the Schrödinger eqn. (5.3) to this form, a suitable change of variable is made; u, v, w and α are expressed in terms of the basic parameters and the two variables β and E. The following expressions are then obtained for Ψ_I, Ψ_{II} and Ψ_{III}.

---

* See Appendix A1

$$\left.\begin{aligned} \Psi_I &= A\, E^*(\alpha_1, -w) + B\, E(\alpha_1, -w) \\ \Psi_{II} &= C\, U(\alpha_2, v) + D\, V(\alpha_2, v) \\ \Psi_{III} &= T\, E(\alpha_3, w) \end{aligned}\right\} \quad (5.6)$$

5.1.2 Results of the Calculations Performed by Cramer and Nix

The penetrability is conveniently expressed as

$$P(E) = \left(\frac{\omega_3}{\omega_1}\right)^{\frac{1}{2}} \left|\frac{T}{A}\right|^2 \quad (5.7)$$

The wave amplitude ratio is determined by requiring that the wave functions and their first derivatives with respect to β be continuous at a and b. The four linear equations obtained are then solved using Cramer's rule [47] and yield

$$\frac{T}{A} = \frac{v'w'\, W\left[E^*(\alpha_1,-w), E(\alpha_1,-w)\right] W\left[U(\alpha_2,v), V(\alpha_2,v)\right]}{\begin{vmatrix} E_a(\alpha_1,-w) & -V_a(\alpha_2,v) & -U_a(\alpha_2,v) & 0 \\ -w' E_a^{(-w)}(\alpha_1,-w) & -v' V_a^{(v)}(\alpha_2,v) & -v' U_a^{(v)}(\alpha_2,v) & 0 \\ 0 & V_b(\alpha_2,v) & U_b(\alpha_2,v) & -E_b(\alpha_3,w) \\ 0 & v' V_b^{(v)}(\alpha_2,v) & v' U_b^{(v)}(\alpha_2,v) & -w' E_b^{(w)}(\alpha_3,w) \end{vmatrix}} \quad (5.8)$$

The primes on the variables v , V and w indicate differentiation with respect to the deformation parameter β , the symbol W denotes the Wronskians of the indicated functions. The subscripts a and b on the parabolic cylinder functions indicate the points where the functions are evaluated. First order differentiation with respect to the argument v , V or w is indicated by a superscript inside parentheses.

5.2 OUR GENERALIZATION OF CRAMER AND NIX[45] METHOD

5.2.1 The Sharp Drop Approximation

We generalize the Cramer and Nix [45] method by removing any restriction on the reflection coefficient R in Region III of the potential barrier. We take R different from zero. Hence, we have a fourth region, in addition to the regions considered by Cramer and Nix.[45] This introduces two more wave functions into the formalism, one more in Region III, a reflected wave and another one in the fourth region, representing the wave transmitted through the barrier. The transmitted wave far from the barrier is a positive complex exponential. We now face the problem of matching the transmitted wave to the solutions of the Schrödinger equation in Region III. We readily notice that Cramer and Nix [45] have matched the wave functions at points a and b , completely defined in terms of the six basic parameters. This matching is independent of

the two variables β and E . Hence, the matching is valid at any energy and any deformation contrary to the J.W.K.B. connections performed at a specific incident energy. To ensure the homogeneity of the formalism, a way has to be found to match the wave functions in Region III and IV independent of β and E .

The top of barrier B , defined by the coordinates β_3 and E_3 is most likely to satisfy our needs; indeed β_3 is completely defined in terms of the six basic parameters. matching at the point (β_3, E_3) would ensure homogeneity. But the potential does not go to zero after the top of barrier B , and the transmitted wave in the form of a complex exponential would be a bad approximation to the central wavefunction. Therefore, we use approximation by letting the potential drop sharply to zero as indicated in Fig. 5.2 This approximation, which will be called the "Sharp Drop Approximation" for obvious reasons, ensures that the matching of functions at (β_3, E_3) is valid for any energy E and any deformation β . Due to the Sharp Drop Approximation, the complex exponential is now a good solution. Smooth matching is secured if the wave functions and their first derivatives are continuous at the point (β_3, E_3).

5.2.2 Potential Energy and Solutions to Schrödinger Equation

The parametrization of the fission barrier under the Sharp-Drop Approximation is defined by Fig. (5.2).

$V(\beta)$ is written as

$$\left.\begin{aligned} V(\beta) &= E_1 - \tfrac{1}{2}\mu\omega_1^2(\beta-\beta_1)^2 && 0 \le \beta \le a \\ &= E_2 + \tfrac{1}{2}\mu\omega_2^2(\beta-\beta_2)^2 && a \le \beta \le b \\ &= E_3 - \tfrac{1}{2}\mu\omega_3^2(\beta-\beta_3)^2 && b \le \beta \le \beta_3 \\ &= 0 && \beta \ge \beta_3 \end{aligned}\right\} \quad (5.4)$$

and $V(\beta)=0$ at $\beta=0$.

The quantities μ, E_i and ω_i are defined in Section 5.1. We choose to connect the three parabolas smoothly by requiring that $V(\beta)$ and its first derivative be continuous at points a and b. This reduces the number of parameters required to completely specify the potential energy of deformation from nine to seven. In addition, the potential is translationally invariant,[45] and this is used to reduce further the number of parameters to six. Hence the parameters are as before the three energies E_i and the three frequencies ω_i. This parameterization yields

$$\beta_1 = \left(2E_1/\mu\omega_1^2\right)^{\frac{1}{2}}$$

$$\left.\begin{aligned} a &= \beta_1 + \left[2(E_1-E_2)/\mu\omega_1^2\right]^{\frac{1}{2}}\left(1+\frac{\omega_1^2}{\omega_2^2}\right)^{-\frac{1}{2}} \\ \beta_2 &= a + \left[2(E_1-E_2)/\mu\omega_2^2\right]^{\frac{1}{2}}\left(1+\frac{\omega_2^2}{\omega_1^2}\right)^{-\frac{1}{2}} \\ b &= \beta_2 + \left[2(E_3-E_2)/\mu\omega_2^2\right]^{\frac{1}{2}}\left(1+\frac{\omega_2^2}{\omega_3^2}\right)^{-\frac{1}{2}} \\ \beta_3 &= b + \left[2(E_3-E_2)/\mu\omega_3^2\right]^{\frac{1}{2}}\left(1+\frac{\omega_3^2}{\omega_2^2}\right)^{-\frac{1}{2}} \end{aligned}\right\} \quad (5.10)$$

As in Section 5.1, μ is assumed to be constant and exact solutions to Schrödinger equation are found. Schrödinger equation is written

$$\left.\begin{aligned}
&\frac{d^2}{d\beta^2}\Psi_I + \frac{2\mu}{\hbar^2}\left[E - E_1 + \tfrac{1}{2}\mu\omega_1^2(\beta-\beta_1)^2\right]\Psi_I = 0 \qquad 0 \le \beta \le a \\
&\frac{d^2}{d\beta^2}\Psi_{II} + \frac{2\mu}{\hbar^2}\left[E - E_2 - \tfrac{1}{2}\mu\omega_2^2(\beta-\beta_2)^2\right]\Psi_{II} = 0 \qquad a \le \beta \le b \\
&\frac{d^2}{d\beta^2}\Psi_{III} + \frac{2\mu}{\hbar^2}\left[E - E_3 + \tfrac{1}{2}\mu\omega_3^2(\beta-\beta_3)^2\right]\Psi_{III} = 0 \qquad b \le \beta \le \beta_3 \\
&\frac{d^2}{d\beta^2}\Psi_{IV} + \frac{2\mu E}{\hbar^2}\Psi_{IV} = 0 \qquad \beta \ge \beta_3
\end{aligned}\right\} \quad (5.11)$$

Again we choose the case for initial momentum transfer from left to right and lift the degeneracy associated with the one-dimensional Schrödinger equations. These equations yield the solutions

$$\left.\begin{aligned}
&\Psi_I = A\,\psi_1(\rightarrow) + B\,\varphi_1(\leftarrow) && 0 \le \beta \le a \\
&\Psi_{II} = C\,\delta_2 + D\,\eta_2 && a \le \beta \le b \\
&\Psi_{III} = F\,\psi_3 + G\,\varphi_3 && b \le \beta \le \beta_3 \\
&\Psi_{IV} = T\,\psi_4(\rightarrow) && \beta \ge \beta_3
\end{aligned}\right\} \quad (5.12)$$

It should be noted that G is different from zero, i.e., the reflection coefficient in Region III is different from zero, and the wave incident on the barrier has unit amplitude. Furthermore, the arrows indicate the direction of the phase velocity. The direction is only needed for ψ_1, φ_1, and ψ_4 since only the amplitudes related to these functions will come in explicitly in the penetrability formula.

The wave function Ψ_{IV} is readily expressed as

$$\Psi_{IV} = T \exp(ik\beta) \tag{5.13}$$

where $k = \left(\frac{2\mu E}{\hbar^2}\right)^{\frac{1}{2}}$ and T is the transmission coefficient. We must now look more closely into the solutions of Schrödinger equation in Region I, II and III. In these regions, it represents a general class of second-order differential equations in the form

$$\left.\begin{aligned} &\frac{d^2y}{du^2} + \left(\tfrac{1}{4}u^2 - \alpha\right) y = 0 \qquad 0 \le \beta \le a \\ &\frac{d^2y}{dv^2} - \left(\tfrac{1}{4}v^2 + \alpha\right) y = 0 \qquad a \le \beta \le b \\ &\frac{d^2y}{dw^2} + \left(\tfrac{1}{4}w^2 - \alpha\right) y = 0 \qquad b \le \beta \le \beta_3 \end{aligned}\right\} \tag{5.14}$$

To express eqns. (5.11) in the above form the following substitutions are needed

$$\left.\begin{aligned} u &= \left(\frac{2\mu\omega_1}{\hbar}\right)^{\frac{1}{2}} (\beta - \beta_1) \qquad \alpha_1 = \frac{E_1 - E}{\hbar\omega_1} \\ v &= \left(\frac{2\mu\omega_2}{\hbar}\right)^{\frac{1}{2}} (\beta - \beta_2) \qquad \alpha_2 = \frac{E_2 - E}{\hbar\omega_2} \\ w &= \left(\frac{2\mu\omega_3}{\hbar}\right)^{\frac{1}{2}} (\beta - \beta_3) \qquad \alpha_3 = \frac{E_3 - E}{\hbar\omega_3} \end{aligned}\right\} \tag{5.15}$$

The solutions of eqns. (5.14) are Weber parabolic cylinder functions.[46] It is essential to select the proper linear combinations of parabolic cylinder functions for the wave functions $\psi_1(\rightarrow)$ and $\varphi_1(\leftarrow)$ to clearly identify the direction of the phase velocity. The asymptotic behaviour of the functions at large values of β indicates the proper linear combination of functions.[48]

The wave functions in Region I are

$$\left.\begin{aligned} \psi_1(\rightarrow) &= E^{*}(\alpha_1, -u) \\ \varphi_1(\leftarrow) &= E\ (\alpha_1, -u) \end{aligned}\right\} \qquad (5.16)$$

where

$$E(\alpha, x) = k_1^{-i}\, W(\alpha, x) + i\, k_1^{i}\, W(\alpha, -x) \qquad (5.17)$$

of the fundamental parabolic cylinder function $W(\alpha, x)$ and k_1 is

$$k_1 = \left(1 + e^{2\pi\alpha}\right)^{i} - e^{\pi\alpha} \qquad (5.18)$$

In Region II, the solutions to eqn. (5.11) can be written in the form of the standard parabolic-cylinder functions U and V of the differential eqn. (5.14), namely

$$\delta_2 = U(\alpha_2, v) \quad ; \quad \eta_2 = V(\alpha_2, v) \qquad (5.19)$$

In Region III, the solutions to eqn. (5.11) can be written in the form of the standard parabolic cylinder functions $W(\alpha, \omega)$ and $W(\alpha, -\omega)$ of eqn. (5.14), namely

$$\psi_3 = W(\alpha_3, \omega) \quad ; \quad \varphi_3 = W(\alpha_3, -\omega) \tag{5.20}$$

The wave functions are conveniently evaluated in practice by the use of their own series expansion.

5.2.3 Penetrability Calculations

The probability current being conserved, we have

$$\left.\begin{aligned} P(E) &= \frac{|j_{TRANS}|}{|j_{INC}|} \frac{|\psi_{TRANS}|^2}{|\psi_{INC}|^2} \\ P(E) &= \frac{|j_{TRANS}|}{|j_{INC}|} \left|\frac{T}{A}\right|^2 \end{aligned}\right\} \tag{5.21}$$

We now find expressions for j_{TRANS} and j_{INC}. The probability current is generally defined by the equation

$$j = -\frac{\hbar}{2\mu i}\left[\left(\frac{d}{d\beta}\psi^*\right)\psi - \left(\frac{d}{d\beta}\psi\right)\psi^*\right] \tag{5.22}$$

Hence

$$j_{TRANS} = -\frac{\hbar}{2\mu i}\left[-ik\, e^{-ikx} e^{ikx} - ik\, e^{ikx} e^{-ikx}\right]$$
$$= \frac{\hbar k}{\mu} \qquad (5.23)$$
$$k = \left(\frac{2\mu E}{\hbar^2}\right)^{\frac{1}{2}}$$

$$j_{INC} = +\frac{\hbar}{2\mu i}\left[\left\{\frac{d}{dE} E^*(\alpha_1, -\omega)\right\} E(\alpha_1, -\omega) - \left\{\frac{d}{dE} E(\alpha_1, -\omega)\right\} E^*(\alpha_1, -\omega)\right]$$
$$= -\frac{\hbar}{2\mu i}\, 2i\, \frac{d\mu}{d\beta} \qquad (5.24)$$
$$= \frac{\hbar}{\mu}\left(\frac{2\mu\omega_1}{\hbar}\right)^{\frac{1}{2}}.$$

Substituting eqn. (5.23) for j_{TRANS} and eqn. (5.24) for j_{INC}, we obtain

$$\frac{|j_{TRANS}|}{|j_{INC}|} = \left(\frac{E}{\hbar\omega_1}\right)^{\frac{1}{2}} \qquad (5.25)$$

This ratio is dimensionless since $\hbar\omega$ has the dimensions of energy. To evaluate T/A, we use the fact that the wave functions and their first derivatives must be continuous at the points a and b. This yields the set of equations (in the notation of Section 5.1)

$$A E_a^{*}(x_1,-\omega) + B E_a(x_1,-\omega) = C U_a(x_2,\nu) + D V_a(x_2,\nu)$$

$$A\left[-\omega' E_a^{*(-\omega)}(x_1,-\omega)\right] + B\left[-\omega' E_a^{(-\omega)}(x_1,-\omega)\right] = C\nu' U_a^{(\nu)}(x_2,\nu) +$$

$$+ D\nu' V_a^{(\nu)}(x_2,\nu)$$

$$C U_b(x_2,\nu) + D V_b(x_2,\nu) = F W_b(x_3,\omega) + G W_b(x_3,\omega)$$

$$C\left[\nu' U_b^{(\nu)}(x_2,\nu)\right] + D\left[\nu' V_b^{(\nu)}(x_2,\nu)\right] = F\left[\omega' W_b^{(\omega)}(x_3,\omega)\right] +$$

$$+ G\left[-\omega' W_b^{(-\omega)}(x_3,\omega)\right] \qquad (5.26)$$

$$F W_{\beta_3}(x_3,\omega) + G W_{\beta_3}(x_3,-\omega) = T \exp(i k \beta_3)$$

$$F\left[\omega' W_{\beta_3}^{(\omega)}(x_3,\omega)\right] + G\left[-\omega' W_{\beta_3}^{(-\omega)}(x_3,-\omega)\right] =$$

$$= T\left[i k \exp\{i k \beta_3\}\right]$$

The ratio T/A is readily obtained by applying Cramer's Rule[47] to this system of equations. T/A can be expressed as

$$T/A = \left(\frac{D_1}{\Delta}\right)^{-1} \qquad (5.27)$$

where Δ and D_1, are defined below.

$$\Delta = \begin{vmatrix} E_a^*(x_1,-u) & E_a(x_1,-u) & -U_a(x_2,v) & -V_a(x_2,v) & 0 & 0 \\ -u' E_a^{*(u)}(x_1,-u) & -u' E_a^{(u)}(x_1,-u) & -v' U_a^{(v)}(x_2,v) & -v' V_a^{(v)}(x_2,v) & 0 & 0 \\ 0 & 0 & U_b(x_2,v) & V_b(x_2,v) & -W_b(x_3,w) & -W_b(x_3,-w) \\ 0 & 0 & v' U_b^{(v)}(x_2,v) & v' V_b^{(v)}(x_2,v) & -w' W_b^{(w)}(x_3,w) & w' W_b^{(-w)}(x_3,-w) \\ 0 & 0 & 0 & 0 & W_{b_3}(x_3,w) & W_{b_3}(x_3,-w) \\ 0 & 0 & 0 & 0 & w' W_{b_3}^{(w)}(x_3,w) & -w' W_{b_3}^{(-w)}(x_3,-w) \end{vmatrix} \tag{5.28}$$

$$
D_1 = \begin{vmatrix}
E_a(\alpha_1,-w) & -U_a(\alpha_2,v) & -V_a(\alpha_2,v) & 0 & 0 & 0 \\
-w' E_a^{(-w)}(\alpha_1,-w) & -v' U_a^{(v)}(\alpha_2,v) & -v' V_a^{(v)}(\alpha_2,v) & 0 & 0 & 0 \\
0 & U_b(\alpha_2,v) & V_b(\alpha_2,v) & -W_b(\alpha_3,w) & -W_b(\alpha_3,-w) & 0 \\
0 & v' U_b^{(v)}(\alpha_2,v) & v' V_b^{(v)}(\alpha_2,v) & -w' W_b^{(w)}(\alpha_3,w) & w' W_b^{(-w)}(\alpha_3,-w) & 0 \\
0 & 0 & 0 & W_{\beta_3}(\alpha_3,w) & W_{\beta_3}(\alpha_3,-w) & -e^{ik\beta_3} \\
0 & 0 & 0 & +w' W_{\beta_3}^{(w)}(\alpha_3,w) & -w' W_{\beta_3}^{(-w)}(\alpha_3,-w) & -ik\, e^{ik\beta_3}
\end{vmatrix} \tag{5.29}
$$

Δ reduces to a product of Wronskians namely

$$\left.\begin{aligned}\Delta = v'w'w' \Big\{ & W\left[E^*(\alpha_1,-u), E(\alpha_1,-u)\right] \cdot \\ & \cdot W\left[U(\alpha_2,v), V(\alpha_2,v)\right] \cdot W\left[W(\alpha_3,w), W(\alpha_3,-w)\right]\Big\}\end{aligned}\right\} \quad (5.30)$$

u' , v' and w' are known and the values of the Wronskians are all constants.*

$$W\left[E^*(\alpha_1,-u), E(\alpha_1,-u)\right] = 2i \quad (5.31)$$

$$W\left[U(\alpha_2,v), V(\alpha_2,v)\right] = \sqrt{\frac{2}{\pi}} \quad (5.32)$$

$$W\left[W(\alpha_3,w), W(\alpha_3,-w)\right] = 1 \quad (5.33)$$

$$\left.\begin{aligned} u' &= \left(\frac{2\mu\omega_1}{\hbar}\right)^{\frac{1}{2}} \\ v' &= \left(\frac{2\mu\omega_2}{\hbar}\right)^{\frac{1}{2}} \\ w' &= \left(\frac{2\mu\omega_3}{\hbar}\right)^{\frac{1}{2}} \end{aligned}\right\} \quad (5.34)$$

Hence

$$\Delta = 8i\left(\frac{\mu}{\hbar}\right)^{\frac{3}{2}} \left[\frac{\omega_1\omega_2\omega_3}{\pi}\right]^{\frac{1}{2}} \quad (5.35)$$

We write down the final expression for the penetrability.

---

* See Appendix A.1

$$P(E) = \left(\frac{E}{\hbar\omega_1}\right)^{\frac{1}{2}} \frac{u'v'w'\, W[E^*(x_1,-u), E(x_1,-u)]\, W[U(x_2,v), V(x_2,v)]\, W[W(x_3,w), W(x_3,-w)]}{}$$

$$\begin{vmatrix}
E_a(x_1,-u) & -U_a(x_2,v) & -V_a(x_2,v) & 0 & 0 & 0 \\
-u' E_a^{(-u)}(x_1,-u) & -v' U_a^{(v)}(x_2,v) & -v' V_a^{(v)}(x_2,v) & 0 & 0 & 0 \\
0 & U_b(x_2,v) & V_b(x_2,v) & -W_b(x_3,w) & -W_b(x_3,-w) & 0 \\
0 & v' U_b^{(v)}(x_2,v) & v' V_b^{(v)}(x_2,v) & -w' W_b^{(-w)}(x_3,w) & w' W_b^{(-w)}(x_3,-w) & 0 \\
0 & 0 & 0 & W_{\beta_3}(x_3,w) & W_{\beta_3}(x_3,-w) & -e^{ik\beta_3} \\
0 & 0 & 0 & +w' W_{\beta_3}^{(w)}(x_3,w) & -w' W_{\beta_3}^{(-w)}(x_3,-w) & -ik\, e^{ik\beta_3}
\end{vmatrix} \qquad (5.36)$$

CHAPTER VI

DISCUSSION AND CONCLUSION

CHAPTER VI

DISCUSSION AND CONCLUSION

6.1 DISCUSSION

6.1.1 The J.W.K.B. Calculations of the Penetrability

Three expressions have been derived for the penetrability in the J.W.K.B. approximation in Chapter IV. Eqn. (4.18) is obtained using Bohm's connection formulae.[38] It is generally accepted as numerically correct. Analytically, the expression lacks rigor and is therefore short of being correct. Indeed, the bi-directional use of the connection formulae introduces insignificant terms in the coefficients of the J.W.K.B. approximated wave functions in the various potential regions. However, the error is cumulative from one connection point to the next. Furthermore, through the use of the connection formulae indiscriminately, some new significant terms appear which would be absent if the uni-directional connection formulae were used. Indeed, neglecting all the negative exponential terms e^{-K_1} and e^{-K_2} in the denominator of eqn. (4.14) as in eqn. (4.15), we obtain

$$P(E) = \frac{4 P_A P_B}{2 P_A P_B + P_A P_B \cos^2\phi + 16 \cos^2\phi} \qquad (6.1)$$

Comparison with eqn. (4.36) yields the extra terms

$$2 P_A P_B + (P_A + P_B) \cos^2 \phi \qquad (6.2)$$

in the denominator.

These terms are significant terms though mathematically they are superfluous. Eqn. (4.36) has been derived rigorously using a correct and consistent formalism. It stands as the valid J.W.K.B. penetrability expression for a double-hump fission barrier. Fröman's "F-Matrix" formalism [39] yields eqn. (4.65) when the energy is close to the value at the top of the second peak. This expression is very important, since in the case of most of the spontaneous or induced fissions, the incident energy is close to the top of barrier B in Fig. (4.2).[23] Eqns. (4.18) and (4.36) do not apply in this case as they are not valid when the classical turning points are close together. Even if the incident energy corresponds exactly to the top of barrier B, Eqn. (4.65) is the right one to use and it provides a straightforward and satisfactory result for the penetrability. Moreover, resonance energy is usually close to the top of barrier B [24]; hence near or at resonance Eqn. (4.65), derived when the classical turning points lie close together, should be applied.

Let us study more closely the behaviour of the

three expressions for the penetrability through two-peaked fission barriers near or at resonance. At resonance we have

$$\cos\phi = 0 \; ; \; \sin\phi = 1 \tag{6.3}$$

Eqn. (4.18) then becomes

$$P(E) = \frac{4 P_A P_B}{(P_A + P_B)^2} \tag{6.4}$$

This is a maximum in the penetrability and if $P_A = P_B$, then

$$P(E) = 1 \tag{6.5}$$

or the barrier is completely transparent.

At resonance Eqn. (4.36) becomes undetermined since the denominator $4\cos^2\phi$ goes to zero. It is remarkable that the correct analytical expression fails at resonance. However, the product $P_A P_B$ is very small since the quantities $2K_1$ or $2K_2$ are large. Hence, near or at resonance, there is a sharp rise of the penetrability to its maximum value of 1 as the incident energy is varied. The full width at half maximum of the resonance peaks is very narrow.
We gather that the penetrability near or at resonance in this

case would be best expressed as a delta function. Eqn. (4.65), at resonance, becomes

$$P(E) = \frac{P_A P_B}{2 - P_B} \tag{6.6}$$

or if $P_B = \frac{1}{2}$,i.e., if the incident energy coincides with the top of barrier B ,

$$P(E) = \frac{P_A}{3} \tag{6.7}$$

Hence, even if barrier A is totally transparent, Eqn. (6.7) only yields

$$P(E) = \frac{1}{3} \tag{6.8}$$

This would explain the fact that unusually long experimental half-lives could not be accounted for theoretically by Eqn. (4.18).[45] Fission probably occurs at an energy close to the top of the second maximum and in this case, Eqn. (4.65) should be used.

6.1.2 Our Generalization of Cramer and Nix Method

A few theoretical considerations should be sufficient to assert the validity of the method. First of all, the method is an improvement on the Cramer and Nix

method. Cramer and Nix diverge from a realistic physical situation by considering the reflection coefficient to be zero in Region III of barrier B illustrated by Fig. (5.1). We discard this assumption but the fact that the reflection coefficient is no longer zero requires the use of the Sharp Drop Approximation to calculate the penetrability. The steep fall of the potential energy after the top of barrier B is evident from Fig. (6.1). This would indicate that very little error is introduced by the Sharp Drop Approximation. Anyhow, it conforms to the physical situation. It is important at this point, to investigate whether the insertion of two new wave functions and the matching at points (β_3, E_3) introduces any discontinuities in the formalism. The numerator of Eqn. (5.36) is always a constant since the Wronskians of the Weber functions used are either imaginary or real constants. Furthermore, the denominator of Eqn. (5.36) can never have a row or a column of zeros since the Weber functions used never go to zero even if α_1, α_2, and α_3, u, v and w are zero, as is the case for α_3 and w if matching is done at the point (β_3, E_3).

In addition, it does not matter if T/A is real, imaginary or a combination of both, since it is $|T/A|^2$ that enters in the penetrability expression, Eqn. (5.36), and not T/A as such. We note that $P(E, \beta)$ is left a completely general expression, since the "Sharp Drop Approximation" does not impose any constraints on E or β.

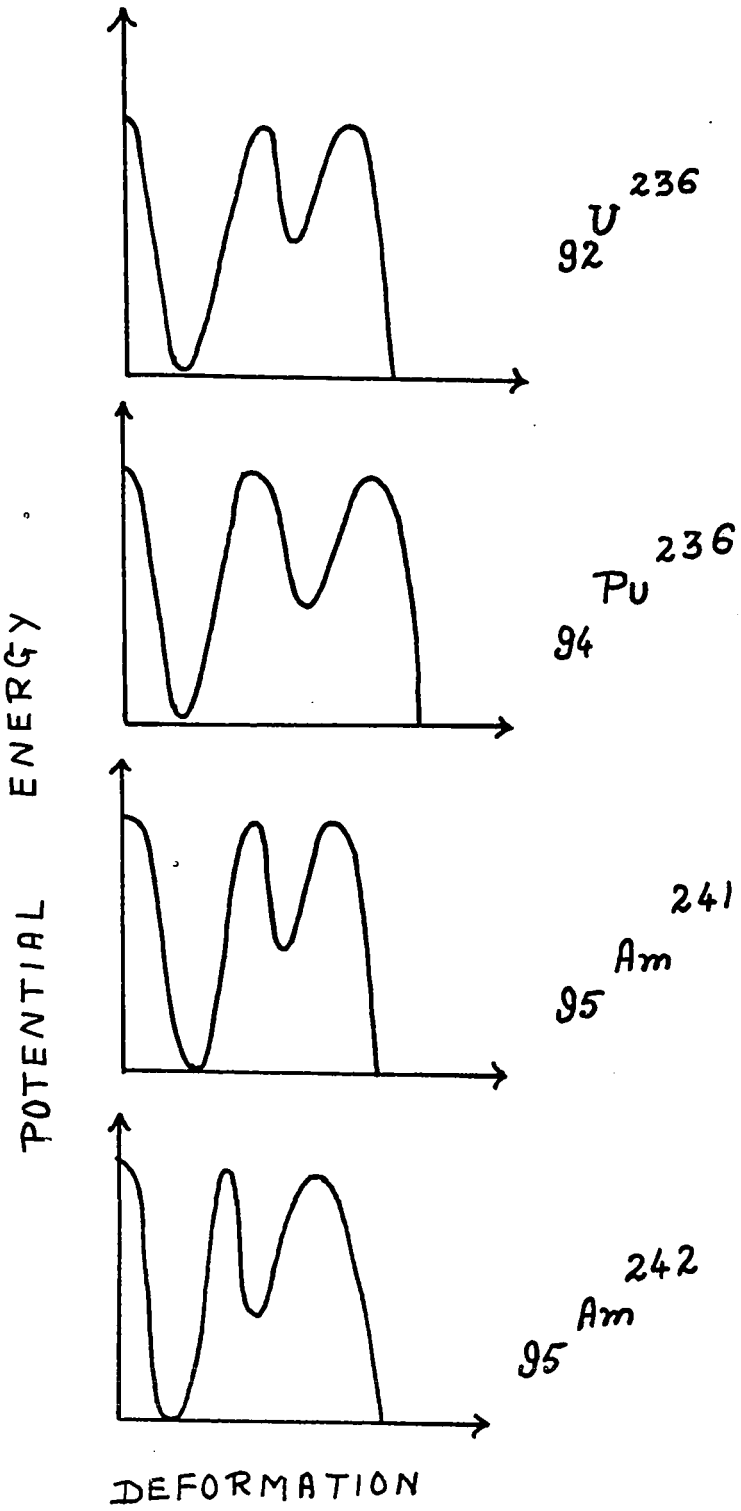

FIG. 6.1 Barrier Functions As Calculated By Strutinsky for Several Heavy Nuclei

6.2 CONCLUSIONS

It was seen in Section 6.1, that the correct expression in eqn. (4.36) for the penetrability calculated with the J.W.K.B. method fails near or at resonance. It is unfortunate, however, that for the sake of numerical agreement of results, researchers did not tackle the problem in depth and sacrificed mathematical rigor. It would be interesting, for instance, to apply Fröman's "F-Matrix" formalism to Strutinsky's barrier parametrized by three or more smoothly joined parabolas, in this case, the expression for $\underset{\sim}{F}(x_1, x_2)$ is given by eqn. (3.32). It is hoped that this would lift, as it did in the case of energy close to the top of barrier B, the discontinuity in the J.W.K.B. expression for the penetrability in eqn. (4.18) without any loss of mathematical rigor. Fröman's "F-Matrix" formalism would also be of help in calculating the penetrability when the incident energy is that corresponding to the bottom of the intermediate well.

Our extension of the Cramer and Nix method to Region IV of the potential energy curve of Fig. (5.6) is only one of the modifications that could be fitted to the method. In the same way, one could also include the first potential minimum of Strutinsky's fission barrier in the Cramer and Nix formalism.

Moreover, through computation the validity of the

"Sharp Drop Approximation" could be tested against Cramer and Nix method. The various expressions obtained for the penetrability in the J.W.K.B. approximation may also be compared to Cramer and Nix method in their respective range of validity and to our generalization of their method. Finally, it would be interesting to test Eqn. (4.18) and Eqn. (4.36) against each other away from resonances. This would involve the use of the computer and the writing of long , extensive and tedious programs and this we would prefer to leave for future research. Nevertheless, after having computed penetrabilities, it would be a must to calculate half-lives and test the theoretical results against experimental ones and assess the validity of our conclusions.

APPENDIX A.1

WEBER PARABOLIC CYLINDER FUNCTIONS

APPENDIX A.1

WEBER PARABOLIC CYLINDER FUNCTIONS

A1.1 SECTION 1

The equation

$$\frac{d^2y}{dx^2} - \left(\tfrac{1}{4}x^2 + a\right) y = 0 \qquad \text{(A1.1)}$$

A1.1.1 Power Series

Even and odd solutions are given by

$$\left.\begin{aligned} y_1 &= e^{-\frac{1}{4}x^2}\left\{1 + \left(a+\tfrac{1}{2}\right)\frac{x^2}{2!} + \left(a+\tfrac{1}{2}\right)\left(a+\tfrac{5}{2}\right)\frac{x^4}{4!} + \cdots\right\} \\ &= e^{\frac{1}{4}x^2}\left\{1 + \left(a-\tfrac{1}{2}\right)\frac{x^2}{2!} + \left(a-\tfrac{1}{2}\right)\left(a-\tfrac{5}{2}\right)\frac{x^4}{4!} + \cdots\right\} \end{aligned}\right\} \qquad \text{(A1.2)}$$

$$\left.\begin{aligned} y_2 &= e^{-\frac{1}{4}x^2}\left\{x + \left(a+\tfrac{3}{2}\right)\frac{x^3}{3!} + \left(a+\tfrac{3}{2}\right)\left(a+\tfrac{7}{2}\right)\frac{x^5}{5!} + \cdots\right\} \\ &= e^{\frac{1}{4}x^2}\left\{x + \left(a-\tfrac{3}{2}\right)\frac{x^3}{3!} + \left(a-\tfrac{3}{2}\right)\left(a-\tfrac{7}{2}\right)\frac{x^5}{5!} + \cdots\right\} \end{aligned}\right\} \qquad \text{(A1.3)}$$

These series are convergent for all values of x .

It is convenient to have a notation for the functions

$$Y_1 = \frac{1}{\sqrt{\pi}}\,\frac{\Gamma\left(\frac{1}{4}-\frac{a}{2}\right)}{2^{\frac{a}{2}+\frac{1}{4}}}\,y_1 = \sqrt{\pi}\,\frac{\sec\pi\left(\frac{1}{4}+\frac{a}{2}\right)}{2^{\frac{1}{2}a+\frac{1}{4}}\,\Gamma\left(\frac{3}{4}+\frac{1}{2}a\right)} \qquad \text{(A1.4)}$$

$$Y_2 = \frac{1}{\sqrt{\pi}}\,\frac{\Gamma\left(\frac{3}{4}-\frac{a}{2}\right)}{2^{\frac{a}{2}-\frac{1}{4}}}\,y_2 = \sqrt{\pi}\,\frac{\operatorname{cosec}\pi\left(\frac{1}{4}+\frac{1}{2}a\right)}{2^{\frac{1}{2}a+\frac{1}{4}}\,\Gamma\left(\frac{1}{4}+\frac{1}{2}a\right)} \qquad \text{(A1.5)}$$

A1.1.2 Standard Solutions

The fundamental solutions of (A1.1) are taken to be $U(a,x)$ and $V(a,x)$ defined by

$$U(a,x) = \cos\pi\left(\tfrac{1}{4}+\tfrac{1}{2}a\right)\cdot Y_1 - \sin\pi\left(\tfrac{1}{4}+\tfrac{1}{2}a\right)\cdot Y_2 \qquad \text{(A1.6)}$$

$$V(a,x) = \frac{1}{\Gamma\left(\frac{1}{2}-a\right)}\left\{\sin\pi\left(\tfrac{1}{4}+\tfrac{a}{2}\right)\cdot Y_1 + \cos\pi\left(\tfrac{1}{4}+\tfrac{a}{2}\right)\cdot Y_2\right\} \qquad \text{(A1.7)}$$

A1.1.3 Wronskians

$$U(a,x)\frac{d}{dx}V(a,x) - V(a,x)\frac{d}{dx}U(a,x) = \sqrt{\frac{2}{\pi}} \qquad \text{(A1.8)}$$

$$U(a,x)\frac{d}{dx}\bar{U}(a,x) - \bar{U}(a,x)\frac{d}{dx}U(a,x) = \sqrt{\frac{2}{\pi}}\,\Gamma\left(\tfrac{1}{2}-a\right) \qquad \text{(A1.9)}$$

$$\bar{V}(a,x)\frac{d}{dx}V(a,x) - V(a,x)\frac{d}{dx}\bar{V}(a,x) = \sqrt{\frac{2}{\pi}}\,\frac{1}{\Gamma\left(\frac{1}{2}-a\right)} \qquad \text{(A1.10)}$$

$$U(a,x)\frac{d}{dx}U(a,-x) - U(a,-x)\frac{d}{dx}U(a,x) = \frac{\sqrt{2\pi}}{\Gamma\left(\frac{1}{2}+a\right)} \qquad \text{(A1.11)}$$

where $\bar{U}$ and $\bar{V}$ are obtained from U and V, the standard solutions.

A1.2 SECTION 2

The equation

$$\frac{d^2y}{dx^2} + \left(\frac{1}{4}x^2 - a\right) y = 0 \qquad \text{(A1.12)}$$

A1.2.1 Power Series

Even and odd solutions of the equations are given by

$$y_1 = e^{-\frac{1}{4}ix^2}\left\{1 + (a+\tfrac{1}{2})\frac{x^2}{2!} + (a+\tfrac{1}{2}i)(a+\tfrac{5}{2}i)\frac{x^4}{4!} + \ldots.\right\} \qquad \text{(A1.13)}$$

$$y_2 = e^{-\frac{1}{4}ix^2}\left\{x + (a+\tfrac{3}{2}i)\frac{x^3}{3!} + (a+\tfrac{3}{2}i)(a+\tfrac{7}{2}i)\frac{x^5}{5!} + \ldots..\right\} \qquad \text{(A1.14)}$$

the series being convergent for all values of x .

A1.2.2 Standard Solutions

The fundamental solutions of (A1.11) are taken to be $W(a,x)$ and $W(a,-x)$ defined by

$$W(a,\pm x) = \frac{(\cosh \pi a)^{\frac{1}{4}}}{2\sqrt{\pi}}\left(G_1 y_1 \pm G_2 y_2\right) \qquad \text{(A1.15)}$$

$$= 2^{-\frac{3}{4}}\left(\sqrt{\frac{G_1}{G_2}}\, y_1 \mp \sqrt{\frac{2G_2}{G_1}}\, y_2\right) \qquad \text{(A1.16)}$$

where

$$G_1 = \left| \Gamma\left(\tfrac{1}{4} + \tfrac{1}{2} i a\right) \right| \quad , \quad G_3 = \left| \Gamma\left(\tfrac{3}{4} + \tfrac{1}{2} i a\right) \right| \qquad \text{(A1.17)}$$

It is convenient to introduce the complex solutions

$$E(a,x) = k^{-\frac{1}{2}} W(a,x) + i k^{\frac{1}{2}} W(a,-x) \qquad \text{(A1.18)}$$

$$\bar{E}(a,x) = \sqrt{\tfrac{1}{2}\left|\Gamma\left(\tfrac{1}{2} + ia\right)\right|}\; E(a,x) \qquad \text{(A1.19)}$$

when

$$k = \sqrt{1 + e^{2\pi a}} - e^{\pi a} \quad , \quad \frac{1}{k} = \sqrt{1 + e^{2\pi a}} + e^{\pi a} \qquad \text{(A1.20)}$$

A1.2.3 Wronskians

$$W(a,x) \frac{d}{dx} W(a,-x) - W(a,-x) \frac{d}{dx} W(a,x) = 1 \qquad \text{(A1.22)}$$

$$E(a,x) \frac{d}{dx} E^*(a,x) - E^*(a,x) \frac{d}{dx} E(a,x) = -2i \qquad \text{(A1.23)}$$

$$\bar{E}(a,x) \frac{d}{dx} \bar{E}^*(a,x) - \bar{E}^*(a,x) \frac{d}{dx} \bar{E}(a,x) = -i \sqrt{\frac{\pi}{\cosh \pi a}} \qquad \text{(A1.24)}$$

REFERENCES

REFERENCES

1) Hahn, O., and Strasseman, F., Naturwiss. 27, 11, (1939)

2) Meitner, L., and Frisch, O.R., Nature, 143,239, (1939)

3) Katchoff, S., Nucleonics 16, 78, (1958).

4) Tsiang, Tsien San, Wei, Ho Zah, Vigneron, R. and Chastel, L., Phys. Rev. 71, 382, (1947).

5) Flerov, G.N. and Petrzhak, K.A., Compt. Rend. USSR, 28, 500,(1940).

6) Libby, W.F., Phys. Rev. 55, 1269,(1939).

7) Bohr, N., and Wheeler, J.A., Phys. Rev. 56,426,(1939).

8) Green, A.E.S., Phys. Rev. 95, 1006,(1954).

9) Swiatecki, W.J., Proc. 2nd.Int. Conf. on Peaceful Uses of Atomic Energy (U.N., Geneva), Vol.15, 248, (1958).

10) Hill, D.L., and Wheeler, J.A., Phys. Rev. 89, 1102, (1953).

11) Rainwater, J., Phys. Rev. 79, 432, (1950).

12) Bohr, A. and Mottelson, B.R., Mat. Fys. Medd. Dan. Vid. Selsk, 30, No.1, (1955).

13) Nilsson, S.G., Mat. Fys. Midd. Dan. Vid. Selsk. 29, N. 16, (1955).

14) Wheeler, J.A., Physica, 22, 1103, (1952).

15) Kumar, K., Bull. Am. Phys. Soc. II, 7, 19, (1962).

16) Bohr, A., Proc. Int. Conf. on Peaceful Uses of Atomic Energy, (U.N., New York), Vol. 2, 151, (1956).

17) Goeppert-Mayer, M., Phys. Rev. 74, 235, (1948).

18) Inglis, D.R., Ann. Phys. (New York), 5,1106 (1958).

19) Rugier, R.B., Burgus, W.H., and Trump, R.L., Phys. Rev. 113, 1589, (1959).

20) Strutinsky, V.M., Yad. Fiz. USSR, 3, 114, (1966).

21) Woods, R.D., and Saxon, D.S., Phys. Rev. 95, 577, (1954).

22) Strutinsky, V.M., Nucl. Phys. A95, 420, (1967).

23) Strutinsky, V.M., Nucl. Phys. A122, 1, (1968).

24) Strutinsky, V.M. and Bjørnholm, S., Int. Symp. on Nuclear Structure, (I.A.E.A. Vienna), 421, (1968).

25) Swiatecki, W.J. and Myers, W.R., Nucl. Phys. 81, 1, (1966).

26) Strutinsky, V.M., and Bjørnholm,S., Nucl. Phys. A136, 1, (1964).

27) Weigmann, H., Zeit. Phys. 214,7, (1968).

28) Nix, J.R., and Walker, J.E., Nucl. Phys. A132, 60, (1969).

29) Polikanov, S.M. et al, Exp. Theor. Phys. 42, 1464, (1962).

30) Flerov, G.N. and Polikanov, S.M., Compt. Rend. Congr. Int. Phys. Nucl. (Paris, France), 1, 407, (1964).

31) Lynn, J.E., Int. Symp. on Nuclear Structure, (I.A.E.A., Vienna), 463, (1968).

32) Vorotnikov, P.E., Dubrovina, S.M., Shigin, V.A., and Otroschenko, G.A., Sov. Nucl. Phys. 5, 210, (1967).

33) Kapitza, S.P. et al, ZhETF Pisma 9, 128, (1968).

34) Androsenko, H.D., and Smirenkin, G.N., ZhETF Pisma 9, (1968).

35) Muzichka, Yu. A., Paschkevich, V.V., and Strutinsky, V.M., J.I.N.R. (Dubna), P7-3733, (1967).

36) Nilsson, S.G. et al, Nucl. Phys. A131, 1, (1969).

37) Paschkevich, V.V., J.I.N.R. (Dubna), D-3893, 94, (1968).

38) Bohm, D., Quantum Theory (Constable and Co., London) 284, (1954).

39) Fröman, N. and Fröman, P.O., J.W.K.B. Approximation, (North Holland Publishing Co., Amsterdam, The Netherlands), (1965).

40) Merzbacher, E., Quantum Mechanics, (John Wiley and Sons, Inc., New York, N.Y., U.S.A.) 112, (1961).

41) Messiah, A., Quantum Mechanics, (North Holland Publishing Co., Amsterdam, The Netherlands), 1, 236, (1958).

42) Ignatiuk, A.V., Rabotnov, N.S. and Smirenkin, G.N., Phys. Letters, (The Netherlands), 29B,209, (1969).

43) Kogan, V.I. and Galitskiy, V.M., Problems in Quantum Mechanics, (Prentice-Hall, Inc., Englewood Cliffs, N.J., U.S.A.) VII,(1963).

44) Gai, E.V. et al, Proc. 2nd Symp. on Phys. and Chem. of Fission, (I.A.E.A., Vienna), 337, (1969).

45) Cramer, J.D. and Nix, J.R., Phys. Rev. C., 2,3, 1048, (1970).

46) Miller, J.C.P., Tables of Weber Parabolic Cylinder Functions, (Her Majesty's Stationery Office, London, England) (1955).

47) Sokolnikoff, I.S. and Redheffer, R.M., Mathematics of Physics and Modern Engineering (McGraw-Hill Book Co. Inc., New York, N.Y., U.S.A.) 708, (1968).

48) Miller, J.C.P., Proc. of the Cambridge Philosophical Society, 48, 428, (1952).